

INVESTIGATION OF 9-ANTHRYLDIAZOMETHANE

AS A

FLUORESCENT LABEL FOR NUCLEOTIDES

By

Antoinette L. Vergallito

Submitted in Partial Fulfillment of the Requirements

for the Degree of

Master of Science

in the

Chemistry

Program

YOUNGSTOWN STATE UNIVERSITY

August, 1997

**Abstract****Investigation of 9-Anthryldiazomethane as a Fluorescent Label for Nucleotides**

Antoinette L. Vergallito

Youngstown State University

Currently, biotin is the most used nonradioactive label for nucleotides. This paper examines the use of 9-anthryldiazomethane (ADAM) as an alternate method for labeling nucleotides, extending its use as a fluorescent labeling reagent to include phosphorylated as well as carboxyl containing biomolecules. Adenosine 5'-monophosphate (AMP) was the primary nucleotide investigated. Studies were also conducted on the synthesis and purification of ADAM. A wide variety of techniques were used in this project. Thin layer chromatography was used to monitor reactions. Attempts to separate the mixture after synthesis of ADAM utilized gravity, flash, and high pressure liquid chromatography. Mass spectrometry and  $^{31}\text{P}$  NMR were used to test for the presence of an ADAM-AMP derivative.

INVESTIGATION OF 9-ANTHRYLDIAZOMETHANE

AS A

FLUORESCENT LABEL FOR NUCLEOTIDES

Antoinette L. Vergallito

I hereby release this thesis to the public. I understand this thesis will be housed at the Circulation Desk of the University library and will be available for public access. I also authorize the University or other individuals to make copies of this thesis as needed for scholarly research.

Signature:

Antoinette L. Vergallito 8/25/97  
Antoinette L. Vergallito Date

Approvals:

Michael A. Serra 8/26/97  
Thesis Advisor, Dr. Michael A. Serra Date

Steven M. Schildcrout 9/7/97  
Committee Member, Dr. Steven M. Schildcrout Date

Jeffrey A. Smiley 9/7/97  
Committee Member, Dr. Jeffrey A. Smiley Date

Peter J. Kasvinsky 8/25/97  
Dean of Graduate Studies, Dr. Peter J. Kasvinsky Date

## Acknowledgements

I would like to thank my advisor, Dr. Serra, for his patience, time, and support during the course of this research project and for giving me the opportunity to graduate. I wish him luck in all of his future endeavors.

My sincere thanks goes out to my committee members, Dr. Smiley and Dr. Schildcrout, for their time and effort in revising my thesis and also to all of the YSU faculty and staff members, including Dr. Peter Norris and Tami Kerr, who offered help and advice toward my project.

Most of all, I would like to thank my family and friends. My parents gave me the love, encouragement, and support that made all of my accomplishments possible. All of the YSU graduate students have my deepest thanks, especially Renita, Gretchen, Bill, and Greg, for their friendship and all of the memories.

**Table of Contents**

Title Page	i
Signature Page	ii
Abstract	iii
Acknowledgements	iv
Table of Contents	v
List of Symbols and Abbreviations	vi
List of Figures	ix
Chapters:	
1. Introduction	1
2. Fluorescence	12
3. Experimental	26
4. Results and Discussion	39
5. Conclusion	54
References	58

**List of Symbols and Abbreviations**

DIG	Digoxigenin
DNA	Deoxyribonucleic acid
RNA	Ribonucleic acid
$K_{dis}$	Dissociation constant
UTP	Uridine 5'-triphosphate
dUTP	Deoxyuridine 5'-triphosphate
dATP	Deoxyadenosine 5'-triphosphate
dCTP	Deoxycytidine 5'-triphosphate
ADAM	9-Anthryldiazomethane
HgO	Mercuric oxide
KOH	Potassium hydroxide
$CH_2N_2$	Diazomethane
HPLC	High Pressure Liquid Chromatography
UV	Ultraviolet
$\epsilon_m$	Extinction coefficient
pg	Picogram
$\mu L$	Microliter
SDS	Sodium Dodecyl Sulfate
pmol	Picomole
GLC	Gas Liquid Chromatography
NMR	Nuclear Magnetic Resonance

kJ	Kilojoule
S	Singlet state
T	Triplet state
mL	Milliliter
nm	Nanometer
$\pi$	Pi
$\sigma$	Sigma
u	Upper electronic state
l	Lower electronic state
B	Einstein B-coefficient
$\epsilon(\nu)$	Molar extinction coefficient at wavenumber $\nu$
c	Speed of light
h	Planck's constant
N	Avogadro's number
n	Refractive index
G	Multiplicity factor
M	Mean electronic transition moment
$\theta$	Electronic wavefunction
A	Einstein A-coefficient
$L(\nu)$	Relative fluorescence quantum intensity at wavenumber $\nu$
$\Delta$	Change
NADH	Reduced Nicotinamide Adenine Dinucleotide

M	Molarity
AMP	Adenine 5'-monophosphate
MeOH	Methanol
NaOH	Sodium hydroxide
HCl	Hydrochloric acid
RT	Room temperature
MHz	Megahertz
GC/MS	Gas chromatography/mass spectrometry
KH <sub>2</sub> PO <sub>4</sub>	Potassium dihydrogen phosphate
CTP	Cytidine 5'-triphosphate
AlCl <sub>3</sub>	Aluminum chloride
THF	Tetrahydrofuran
DMPU	1,3-dimethyl-oxo-hexahydropyrimidine
NCS	N-chlorosuccinimide
mmol	Millimole



**List of Figures**

Figure 1	Biotin	2
Figure 2	Biotinylated UTP	3
Figure 3	Photoactive biotin	4
Figure 4	Synthesis of 9-Anthryldiazomethane	4
Figure 5	Mercuric oxide reaction	5
Figure 6	Valence resonance structures of the diazomethane functional group	6
Figure 7	Esterification of carboxylic acids with diazomethane	6
Figure 8	Esterification of fatty acids with ADAM	7
Figure 9	Esterification of amino acids with ADAM	8
Figure 10	Esterification of N-acetylamino acids with ADAM	9
Figure 11	Reaction of diazomethane and phosphonic acid	9
Figure 12	Reaction of oxaphospholene with diazomethane	10
Figure 13	Proposed mechanism for reaction of ADAM and nucleotides	11
Figure 14	Multiplicity	14
Figure 15	Schematic energy-level diagram for a diatomic molecule	15
Figure 16	Excitation and fluorescence emission spectra of 0.3 $\mu\text{g/mL}$ anthracene in methanol	17
Figure 17	Fluorescence/concentration graph for the coenzyme NADH in distilled water solution	23

Figure 18	Proposed reaction of ADAM with AMP	41
Figure 19	Initial $^{31}\text{P}$ NMR Spectrum of Derivative	44
Figure 20	24 Hour $^{31}\text{P}$ NMR Spectrum of Derivative	45
Figure 21	IR of ADAM using manganese dioxide	48
Figure 22	IR of ADAM using mercuric oxide	49
Figure 23	IR of ADAM using NCS	50
Figure 24	TLC of ADAM and anthracene compounds	51
Figure 25	HPLC of ADAM	52
Figure 26	The resonance structures of a) phosphonates and b) monophosphates	56

## Chapter 1

### Introduction

Nonradioactive labeling methods have increasingly been studied to develop specific and sensitive bioanalytical indicator systems to uniformly detect biological molecules such as nucleic acids, proteins, and glycans. Nonradioactive, bioanalytical indicator systems are usually composed of a biological target molecule and a specific binding partner called a probe. The interaction of the two species produces a complex that is directly or indirectly detectable. Such nonradioactive indicator systems are rapidly replacing radioactive labeling methods that use isotopes such as  $^3\text{H}$ ,  $^{32}\text{P}$ ,  $^{14}\text{C}$ ,  $^{35}\text{S}$ , and  $^{125}\text{I}$  incorporated into the molecular structure. The growing interest in nonradioactive labeling arises from several advantages over radioactive methods such as stable modification groups, no accumulation of radioactive waste, and no need for a specialized laboratory and personnel trained in nuclear techniques (1).

There are several kinds of nonradioactive labeling methods for nucleic acids and nucleotides based on enzymatic, photochemical, or chemical incorporation of a binding molecule to the target molecule that can easily be detected by methods such as optical or fluorescence measurements (1). Enzymatic labeling reactions are catalyzed by various polymerases or transferases. For example, nucleotide analogues modified with molecules such as biotin or digoxigenin (DIG) are used instead of or with their non-modified counterparts. This is useful for labeling DNA, RNA, and oligodeoxynucleotides. Photochemical labeling of nucleic acids uses azide-containing compounds which involve the loss of nitrogen, and it is the resulting nitrene intermediate which reacts with the nucleic acid. Finally, chemical derivations can be accomplished by various alternative

reactions such as mercaptan derivatization of amine residues of the nucleotide base by 3-(2-pyridine-dithionic)-propionic acid-hydroxy-succinimide-ester (2).

The most widely used nonradioactive label for nucleic acids is biotin, also known as vitamin H (Figure 1). This method can be divided into enzymatic and photochemical categories. In the enzymatic approach, biotin binds to the nucleic acid. Avidin, a protein isolated from egg white, or streptavidin, a protein isolated from *Streptomyces avidinii* bacteria, is used to bind to the biotinylated nucleic acid because each has a high affinity for biotin. The avidin or streptavidin is conjugated to an enzyme such as alkaline phosphatase and in the presence of a substrate, the enzyme will liberate products that can be measured spectrophotometrically. Thus, the avidin or streptavidin-enzyme complex acts as an indicator for the biotin-labeled nucleic acid (3).

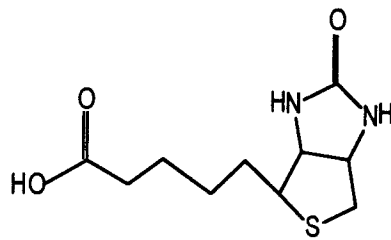


Figure 1. Biotin

Many features make biotin an exceptional label. One factor is that the interaction between biotin and avidin has one of the highest binding constants known ( $K_{dis} = 10^{-15}$ ). Also avidin can be coupled to indicator molecules other than enzymes such as fluorescent dyes or antibodies; thus minute quantities of biotin can be detected (4).

Langer *et al.* (4) were the first to synthesize biotin labeled UTP (Figure 2) and dUTP as substrates for RNA and DNA polymerases. The biotin molecule was attached to the carbon at the 5-position of uridine or deoxyuridine by a linker arm. Evidence for

biotin substitution was that polynucleotides synthesized in the presence of biotin-labeled nucleotides were selectively retained when chromatographed over avidin-Sepharose affinity columns and were immunoprecipitated when treated with anti-biotin antibodies and then with formalin-fixed staphylococcus (4). Later Gebeyehu and colleagues reported the synthesis of biotin dATP and dCTP with a linker arm attached to the N-6 position of adenine and N-4 position of cytosine (5). Biotin-labeled polynucleotides can be useful as affinity probes by nick translation or random primer labeling to detect and isolate specific DNA and RNA sequences (3).

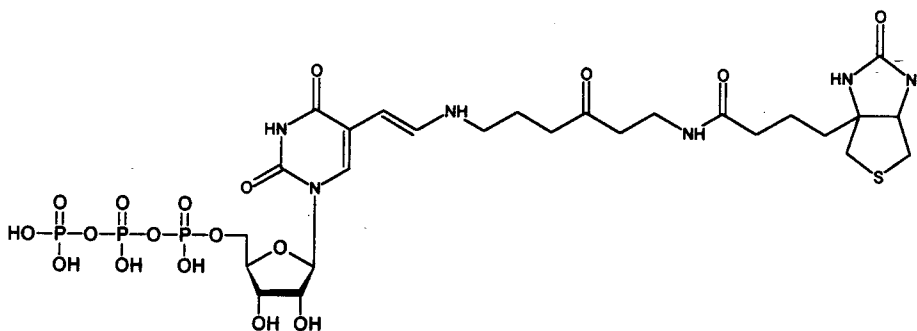


Figure 2. Biotinylated UTP

Photobiotin (Figure 3), a derivative of biotin, has been employed as a photochemical reagent. This reagent contains a photoreactive aryl azide group attached to biotin through a charged linker arm. When irradiated with strong visible light in the presence of DNA, photobiotin covalently links biotin groups to DNA (3). Both methods are routinely used in labeling nucleic acids.

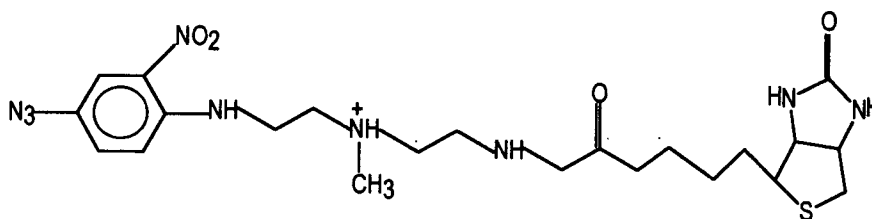


Figure 3. Photoactive biotin

A nucleotide consists of a base, a sugar, and a phosphate group. As described above, the most common nonradioactive method used today, biotin, labels at the carbon or the nitrogen positions of the base. A highly fluorescent compound, 9-anthryldiazomethane (ADAM) (Figure 4), was recently developed to have nonradioactive labeling capabilities by formation of an ester bond. In 1966, Nakaya *et al.* (6) synthesized ADAM from the dehydrogenation of 9-anthraldehyde hydrazone using mercuric oxide as the oxidizing agent (Figure 4). The hydrazone was prepared from 9-anthraldehyde and hydrazine hydrate ( $\text{NH}_2\text{NH}_2 \cdot \text{H}_2\text{O}$ ) (6). The preferred solvent for hydrazone dehydrogenation with  $\text{HgO}$  is ether. Sodium sulfate is used to bind reaction water, and catalytic amounts of alcoholic  $\text{KOH}$  enhance reaction rates. The reaction scheme in

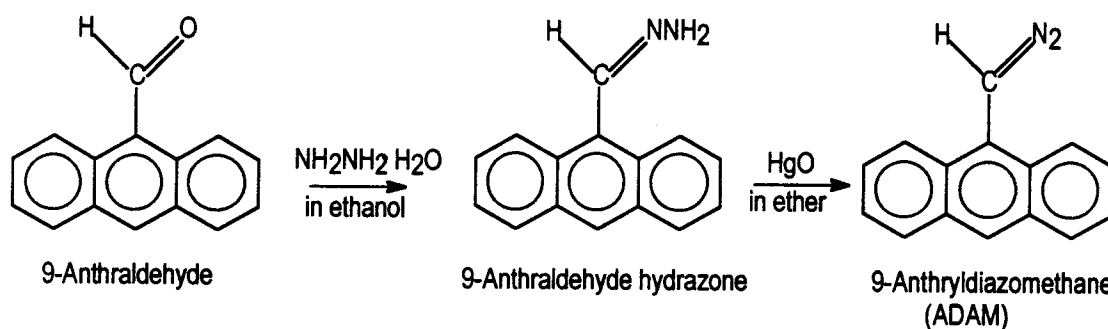


Figure 4. Synthesis of 9-anthryldiazomethane (6)

Figure 5 shows the function of the base in the HgO reaction (7). The 9-anthryldiazomethane crystals were found to decompose at 63-64°C. The infrared spectrum gave a diazo band at 2080  $\text{cm}^{-1}$  (6).

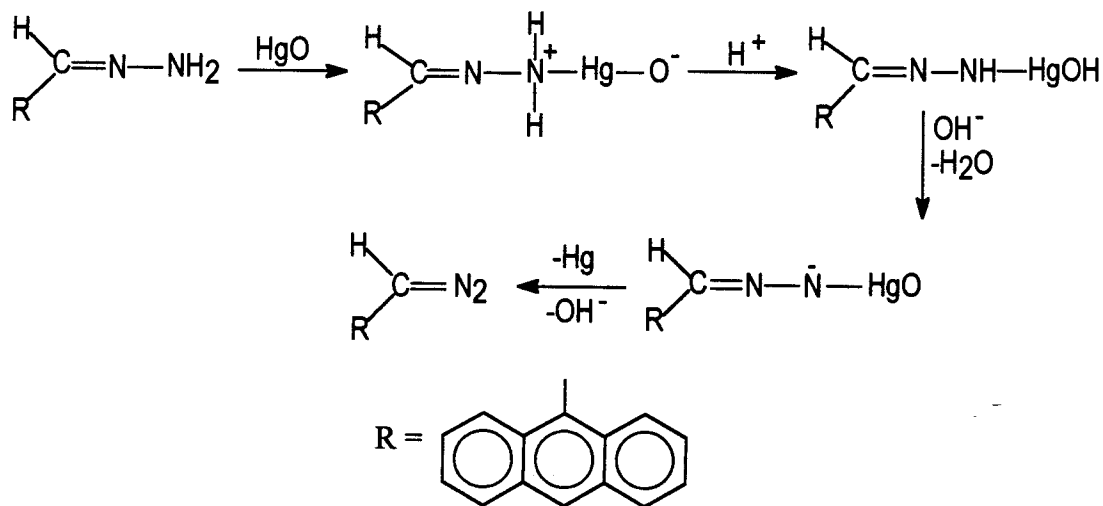


Figure 5. Mercuric oxide reaction

The reactive site on ADAM is the diazomethane functional group. Diazo compounds are usually unstable and decompose rapidly on exposure to light; ADAM displays similar reactivity (8). The diazomethane group of ADAM positioned at carbon 9 on the anthracene has several resonance forms illustrated in Figure 6. Many of the diazo reactions necessarily involve structure 1 because of the negative charge on the carbon which makes it a stronger base (9).

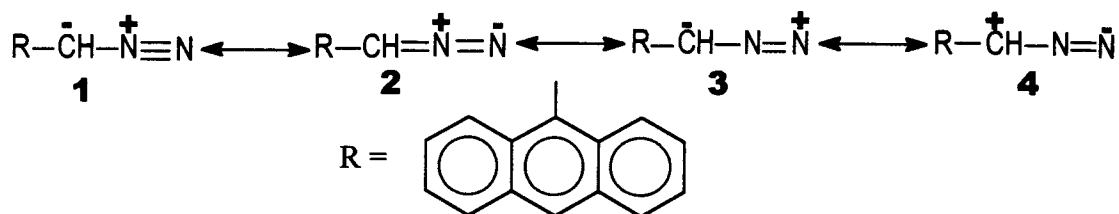


Figure 6. Valence resonance structures of the diazomethane functional group

One of the major reactions that diazo compounds, especially diazomethane ( $\text{CH}_2\text{N}_2$ ), undergo efficiently is converting carboxylic acids to esters in a quick and clean reaction. The carboxylate anion acts as a nucleophile. Since this nucleophile can also act as a base, the reaction conditions must be selected to favor substitution over elimination. In the esterification of carboxylic acids with diazomethane, the alkylating agent is the reactive methyl diazonium ion, which is generated by proton transfer from the carboxylic acid to diazomethane. The resonance form of structure 1 in Figure 6 shows that the negatively charged carbon allows for the abstraction of the proton. The collapse of the resulting ion pair with the loss of nitrogen is extremely rapid (Figure 7). The main drawback of this reaction; however, is the toxicity of diazomethane (10).

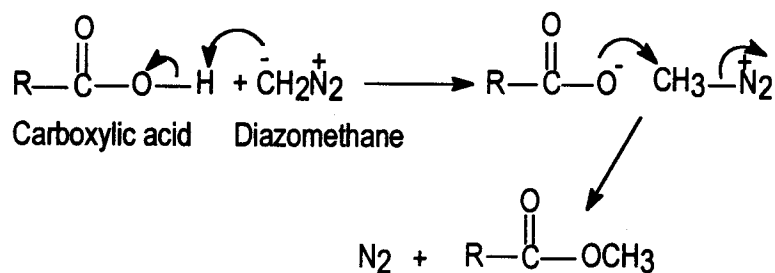


Figure 7. Esterification of carboxylic acids with diazomethane



The use of 9-anthryldiazomethane as a labeling reagent was first reported by Barker and colleagues in 1980 (11). This compound was found to react with carboxyl groups of fatty acids to give ester derivatives as described above with diazomethane. This reaction is shown in Figure 8. The fatty acid ester derivative was analyzed by high pressure liquid chromatography (HPLC) with UV and fluorescence detectors and serial dilutions of the derivatized fatty acids were performed to determine the limits of detection. The extinction coefficient ( $\epsilon_m$ ) for 9-anthracenyl-methylacetate was found to be  $63,000 \text{ M}^{-1} \text{ cm}^{-1}$  at 256 nm. The detection limit of the individual fatty acid esters for fluorescence was  $15 \text{ pg}/\mu\text{L}$  and for ultraviolet spectroscopy was  $150 \text{ pg}/\mu\text{L}$ . Barker and colleagues also studied the preparation and properties of ADAM using activated manganese dioxide instead of mercuric oxide. They discovered that ADAM was unstable when exposed to light at room temperature, however the rate of decomposition was slow (50% within 7 days). Solid ADAM could be stored at  $-76^\circ\text{C}$  in the dark for a month with no significant decomposition (11). Hence, 9-anthryldiazomethane proved to be a new and sensitive method for the quantification of low picomole quantities of fatty acids.

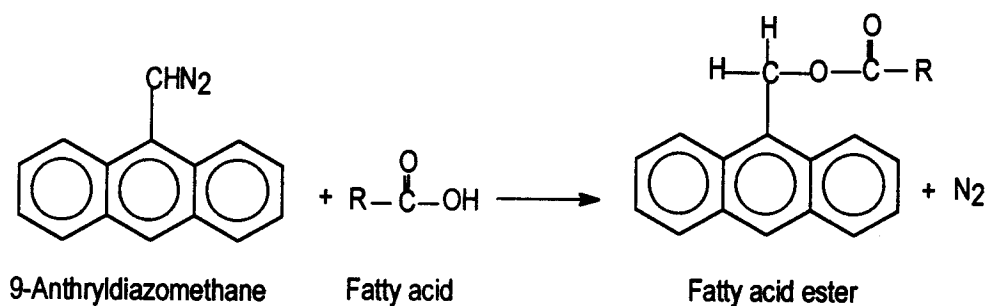


Figure 8. Esterification of fatty acids with ADAM

Yoshida *et al.* (12) took advantage of ADAM's reactivity with carboxylic acids and studied its reaction with the carboxyl groups in amino acids. The general reaction is shown in Figure 9. Preliminary results gave poor yields of amino acid esters which was thought to be due to the zwitterion between the carboxylic and amino groups. In attempts to improve this method, the effect of additives such as the negatively charged detergent sodium dodecyl sulfate (SDS) was studied. Using SDS, which surrounds and masks the positively charged amino group, an elevated reaction temperature of 50°C, and a reaction time of three hours improved yields. The derivatized amino acids were separated by HPLC and the excitation (255 nm) and emission (412 nm) spectra were measured with a fluorescence spectrophotometer (12).

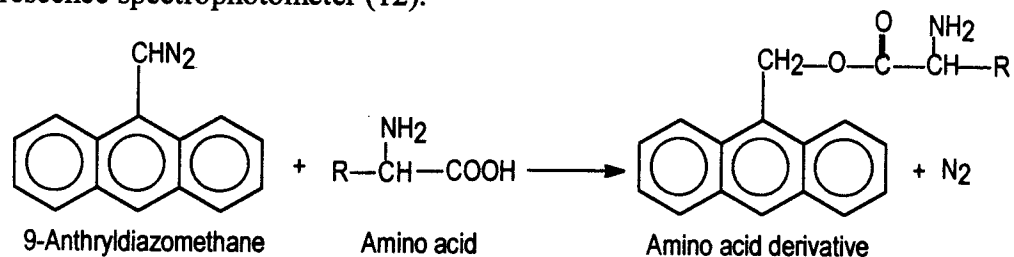


Figure 9. Esterification of amino acids with ADAM

Although yields increased with the use of SDS and elevated temperatures, problems due to the positively charged amino group could not be completely overcome. Using derivatized amino acids in which the amino group is blocked removes the zwitterion character of underivatized amino acids. Labeling of N-acetylamino acids with ADAM was studied by Kawakami *et al.* (13). The reaction proceeded at 30°C for 60 minutes in the dark (Figure 10). It was found that adding silica gel to the reaction, which acted as an inorganic acid, produced good yields since the reaction must occur under

acidic conditions to ensure that the carboxylic acid is protonated. The anthryl esters were separated by HPLC and detected fluorimetrically. Sensitivity of detection ranged from 0.10 pmol for acetyl glutamine to 5.5 pmol for acetyl isoleucine and acetyl leucine. This method proved to be better than other methods in terms of application and sensitivity (13).

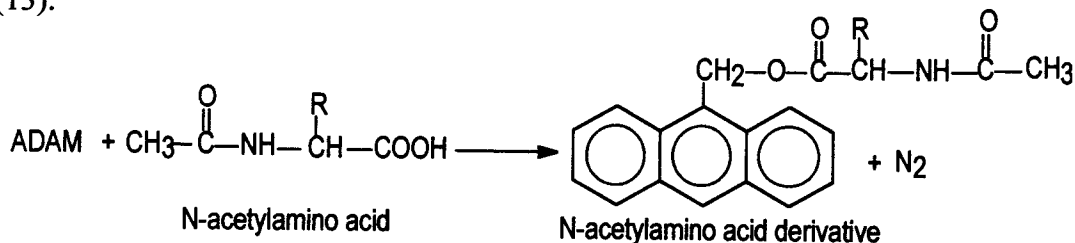


Figure 10. Esterification of N-acetylamino acids with ADAM

ADAM has been used to label carboxyl containing molecules *via* the formation of an ester bond between the carbon of the diazo group and the oxygen of the carboxyl group. We hypothesize that its use as a labeling reagent can be extended to phosphate-containing molecules based on earlier work with diazomethane. In 1977, Macomber (14) demonstrated the reaction of a phosphonic acid in methanol with diazomethane in ether to give the corresponding diester in quantitative yield and >98% purity by GLC and NMR (Figure 11). Oxaphospholene was also derivatized to its methyl ester with >99% purity (Figure 12). Both reactions occurred by simply mixing the two reagents and were instantaneous at room temperature (14).

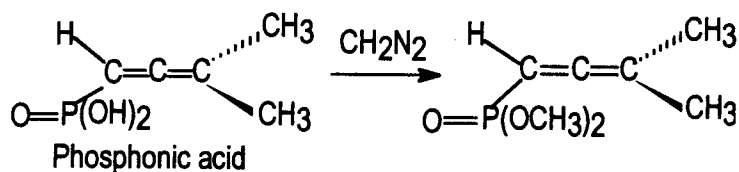


Figure 11. Reaction of diazomethane and phosphonic acid

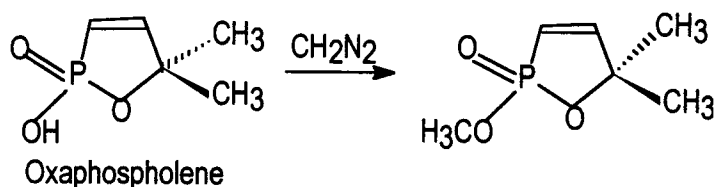
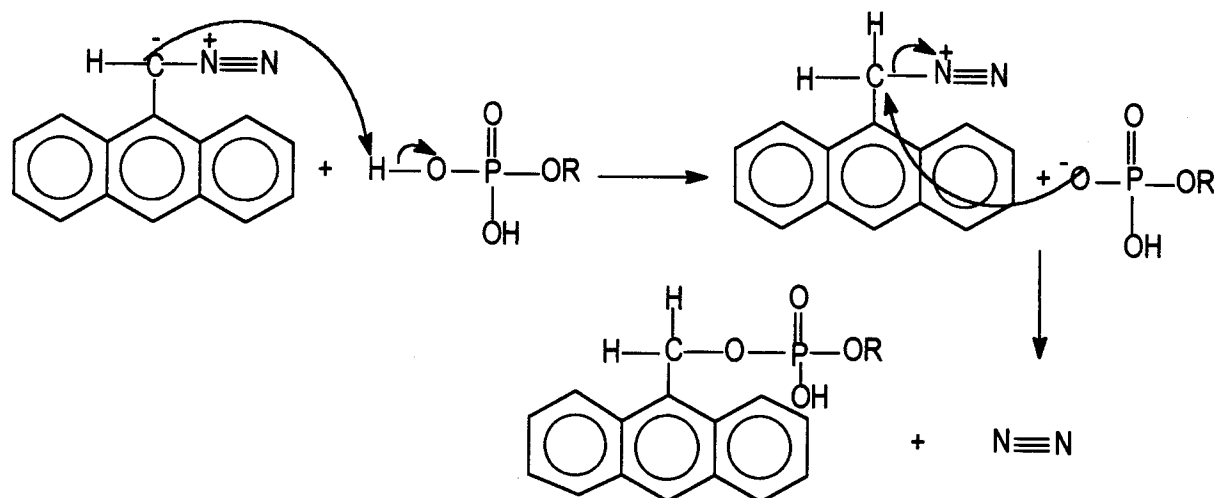


Figure 12. Reaction of oxaphospholene with diazomethane

If diazomethane is capable of reacting to form phosphonate esters, then ADAM should also be able to form phosphonate esters. We reasoned that since phosphates and phosphonates are structurally similar, ADAM could be used to make phosphoester bonds, thereby, fluorescently labeling phosphate containing molecules. According to Carey (10), phosphoesters can produce stable enol phosphates. The proposed mechanism for phosphate ester formation is one that mimics the mechanism of carboxylic acids and diazomethane to produce an ester (Figure 13) (10). Unlike the current nucleotide label, biotin, ADAM could potentially label at the phosphate group instead of the nitrogen or carbon on the base of the nucleotide. The goal of this project is thus to synthesize ADAM and find conditions which lead to the rapid room temperature derivatization of nucleotides and oligonucleotides by the formation of phosphoester bonds. This technique could be applied to all phosphate containing biomolecules, thus, expanding ADAM's use as a nonradioactive, fluorescent label.



R = ribose or deoxyribose and the nitrogenous base

Figure 13. Proposed mechanism for reaction of ADAM and nucleotides

## Chapter 2

### Fluorescence

As proposed in Chapter 1, fluorescent compounds, such as 9-anthryldiazomethane (Figure 4), can be used to label and quantitatively analyze biomolecules present in trace amounts. Fluorescent labeling can provide for easy separation of these biological molecules by thin layer chromatography, high pressure liquid chromatography, and other spectroscopic methods in which the unique fluorescence can be detected.

Why are fluorescent compounds fluorescent to begin with? This is explained by studying the behavior of the electrons in a molecule exposed to electromagnetic radiation (15). In order to fully understand how molecules fluoresce, one must be familiar with the molecular electronic energy levels and the transitions made between them (16).

Analytically useful fluorescence is restricted to compounds possessing large conjugated systems in which the  $\pi$  electrons can be promoted to an antibonding  $\pi$  orbital. Aromatic hydrocarbons, such as 9-anthryldiazomethane, are a group of strongly fluorescent organic compounds since they are highly conjugated (17). However, fluorescence is influenced by structural and environmental factors such as rigidity, solvent, pH, metal ions, and concentration. Also a number of factors can quench fluorescence.

The electrons of a molecule can be excited to higher energy states, and the radiation that is absorbed in the process, or the energy emitted in the return to the ground state, is studied mostly by the use of spectroscopic methods (16). Spectroscopy is the study of absorption and emission of electromagnetic radiation (light) by matter. The set of frequencies absorbed by a sample determines its absorption spectrum; the frequencies emitted provide the emission spectrum (15). Fluorescence spectroscopy is valuable

because it can provide spectra from extremely small amounts of material with high sensitivity and specificity. Fluorescence is a process in which radiation is emitted by molecules or atoms that have been excited by the absorption of radiation (18). The energies involved are generally large, 200-600 kJ/ mol; hence, the electronic spectra of molecules are usually found in the ultraviolet or visible region of the spectrum (16).

Molecular electronic energies are represented by potential energy curves in which the potential energy of each electronic state is plotted as a function of internuclear vibrational coordinate. An electronic energy level is a physically stable state of a molecule if the potential energy curve has a minimum. Most molecules have excited electronic states that are not stable. Excitation to these states leads to dissociation, and the spectrum corresponding to these transitions contains a continuous range of frequencies (16).

According to the Pauli exclusion principle, the spins of two electrons in the same orbital are opposite to each other (paired). A molecule with an even number of electrons typically has all its electrons paired and is said to be in a singlet state. Whether the molecule is in the ground state or excited state, as long as all the electrons are paired, the molecule is in a singlet state, designated  $S_0, S_1, S_2, \dots$ . If all but two electrons in the molecule are paired then it is in a triplet state,  $T_1, T_2, T_3 \dots$  (16). These terms are defined by the concept known as multiplicity, originally derived from the number of lines shown on a spectrum. It is related to the number of unpaired electrons and is given by the expression  $M = 2S + 1$ . S, P, D, and F are states depending upon the orbital angular momentum. Corresponding to states S, P, D, F... are quantum numbers  $L = 0, 1, 2, 3, \dots$ , which parallel the atomic  $l$  values for s, p, d, f... orbitals.  $S = \sum s_i$  where  $s_i$  are the single

electron spin quantum numbers  $\pm 1/2$ . Thus, if  $S = 0$ , the multiplicity is one and the state is called a singlet. If  $S = 1$ , the multiplicity is three and the state is a triplet. For example, consider carbon ( $1s^2 2s^2 2p^2$ ). The two 2p electrons may be paired ( $S=0$ ) or have parallel spins in different orbitals ( $S = 1$ ) (19).

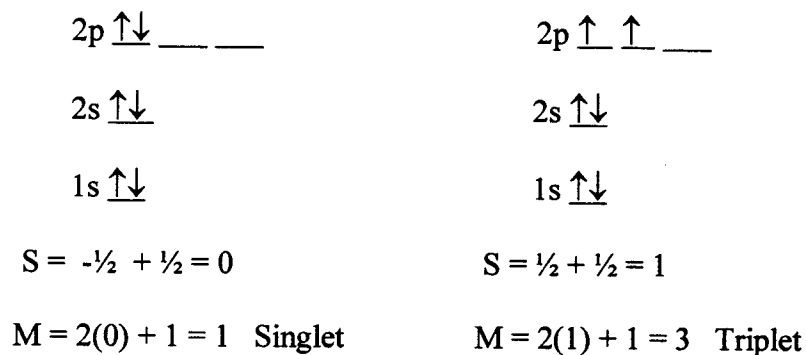


Figure 14. Multiplicity

To absorb radiation, a molecule must first interact with the radiation. This interaction must occur within approximately  $10^{-15}$  s, the period of oscillation of the UV or visible electromagnetic wave. Electronic absorption frequently involves excitation of an electron from the lowest vibrational level of the ground state of a molecule to a higher vibrational level of the first excited state. A vertical line in an energy diagram represents an electronic transition. Also, the electronic levels of molecules are quantized so that the absorption bands can occur only at definite values corresponding to the energies required to promote electrons from one level to another. In Figure 15 an electronic transition in absorption shows a series of closely spaced lines corresponding to different vibrational energies of the upper state (16).



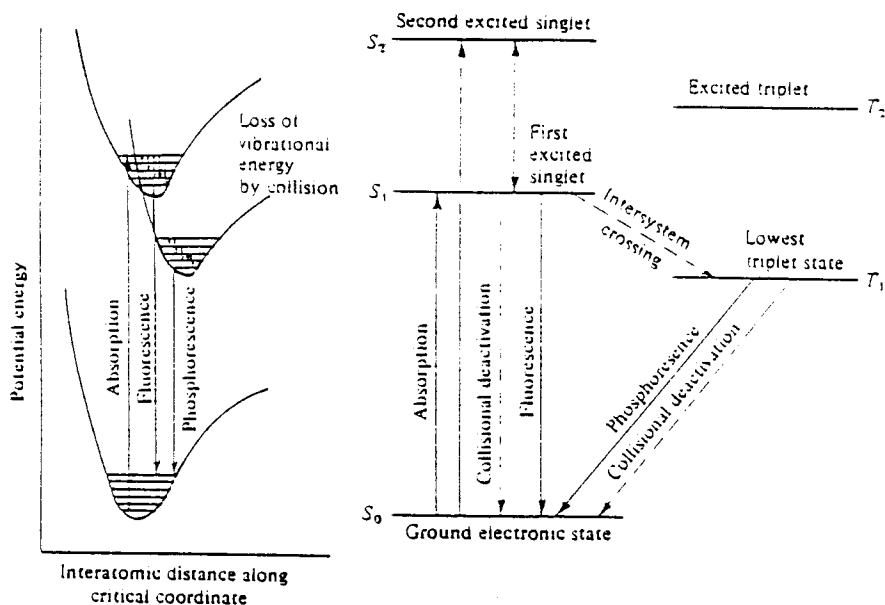


Figure 15. Schematic energy-level diagram for a diatomic molecule. This figure was taken from reference 16.

Absorption terminates when the solute molecule arrives in any one of several possible vibrational levels in an excited electronic state that is still surrounded by the ground state of the solvent molecules. An excited molecule can return to its ground state by any of several paths shown in Figure 15. The favored route is the one that minimizes the lifetime of the excited state. Within  $10^{-12}$  s the electronically excited solute molecule drops to the lowest vibrational level of the lowest excited singlet state by means of radiationless processes, converting the energy to solvent heating. The excess energy is transferred to other molecules through collisions as well as by partitioning the excess energy to other possible modes of vibration or rotation within the excited molecule. The solvent molecules reorient themselves to a state of equilibrium compatible with the new

molecular polarity, following excitation. The vibrational and solvent relaxation processes are accompanied by a gain of thermal energy (16).

When molecules reach the lowest vibrational level of the lowest excited singlet state, the radiation of fluorescence can occur when the molecule returns to any of the vibrational levels of the ground electronic state. If the potential energy curve of the excited singlet state crosses that of the triplet state, some excited molecules may pass over to the lowest triplet state by intersystem crossing that involves vibrational coupling between the excited singlet state,  $S_1$ , and the triplet state,  $T_1$ . After occupation of the triplet state is achieved, the molecule undergoes vibrational relaxation to the lowest excited triplet state. From this state, electromagnetic radiation can be emitted and this is called phosphorescence (16).

Each transition involves radiation of a specific wavelength. The fluorescence radiative process ( $S_1 \rightarrow S_0$ ) has a short natural lifetime ( $10^{-9}$  to  $10^{-7}$  s) so that in many molecules it can compete effectively with other processes capable of removing the excitational energy, such as internal conversion or intersystem crossing. The consequences of this mechanism are twofold. First, since the vibrational levels of both ground and excited states are similar, the fluorescence spectrum approximately mirrors the absorption (or excitation) spectrum (Figure 16). However, because the molecules relax to lower vibrational levels in the excited state and because of the solvent reorientation in the excited state and the ground state, the electromagnetic radiation corresponding to fluorescence is of lower energy than the exciting radiation and therefore appears at longer wavelengths. Second, although the intensity of the fluorescence spectrum depends on the excitation wavelength, its spectral pattern is independent of the

excitation wavelength, due to rapid vibrational relaxation in the first excited state. If the absorption process leads to an electronic state in which the energy exceeds the bond strength of one of the solute's linkages, then excitation energy may be lost by molecular dissociation before fluorescence can occur (16).

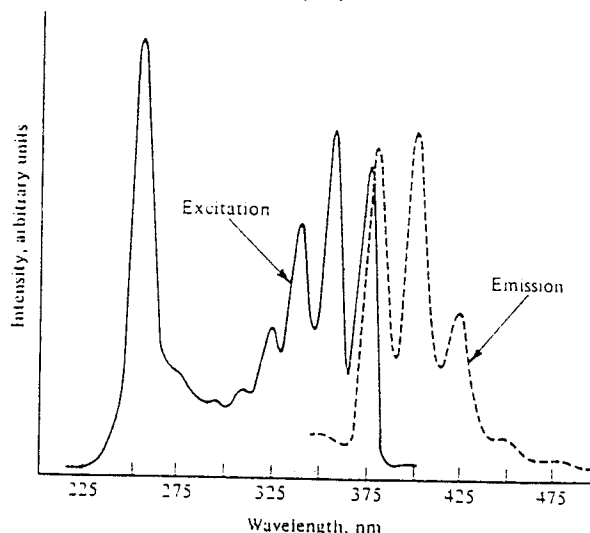


Figure 16. Excitation and fluorescence emission spectra of 0.3  $\mu\text{g/mL}$  anthracene in methanol. This figure was taken from reference 16.

Polyatomic molecules, with a large number of modes of vibration, have a more complicated absorption spectrum and a more complex fluorescence (20). This is because these highly conjugated compounds have  $\pi$  electrons that are less strongly bound within the molecule than  $\sigma$  electrons and can be promoted to  $\pi$  antibonding orbitals by absorption of electromagnetic radiation of low energy without much disruption of bonding. Aromatic hydrocarbons exhibit an intense fluorescence in the ultraviolet or visible region, with fluorescence energies decreasing with increasing yield as the length of the conjugated system is increased (17). Benzene emits in the ultraviolet, and a progression movement of the emission to the visible region occurs through the linear polyacenes with anthracene emitting in the blue, naphthalene in the green, and pentacene

in the red. The quantum yields of fluorescence increase with increased number of rings from a value of 0.28 for benzene to 0.46 for anthracene, then diminish to a low value with pentacene (18).

In aromatic hydrocarbons, the energy of each  $\pi$  electronic excited state, relative to the ground state, and the identification and assignment of the excited state are important information to be determined by spectroscopy (21). The probability that a system will undergo a transition from one state to another under the influence of a time-dependent radiation field was developed by Dirac and is known as the time-dependent perturbation theory (22). For radiative transitions the determination of the magnitude and polarization of the transition moment is important in the assignment of an excited electronic state. For an absorption transition from a lower electronic state,  $l$ , to an upper electronic state,  $u$ , the Einstein B-coefficient for induced absorption is

$$B_{ul} = \frac{2303 c}{h n N} \int \epsilon(\nu) d\nu / \nu = \frac{8 \pi^3 G}{3 h^2} |\bar{M}_{ul}|^2 \quad (\text{Eqn. 1})$$

where  $\epsilon(\nu)$  is the molar extinction coefficient at wavenumber  $\nu$ ,  $c$  is the speed of light,  $h$  is Planck's constant,  $N$  is Avogadro's number,  $n$  is the refractive index of the molecular environment and  $G$  is a multiplicity factor.  $\bar{M}_{ul}$  is the mean electronic transition moment given by

$$\bar{M}_{ul} = \langle \theta_l | \bar{M} | \theta_u \rangle \quad (\text{Eqn. 2})$$

where  $\theta_l$  and  $\theta_u$  are the electronic wavefunctions of  $l$  and  $u$ , respectively, and  $\bar{M}$  is the mean electric dipole operator (21).

For a transition from a higher electronic state  $u$  to a lower electronic state  $l$ , the Einstein A-coefficient for the probability for spontaneous emission of fluorescence is

$$A_{lu} = \frac{64 \pi^4 n^3 G}{3h} \frac{|\bar{M}_{lu}|^2 \int L(\nu) d\nu}{\int L(\nu) d\nu/\nu^3} \quad (\text{Eqn. 3})$$

where  $L(\nu)$  is the relative fluorescence quantum intensity at wavenumber  $\nu$ .  $\bar{M}_{lu}$  is the mean electronic transition moment given by (21)

$$\bar{M}_{lu} = \langle \theta_u | \bar{M} | \theta_l \rangle \quad (\text{Eqn. 4})$$

These two vitally significant coefficients form the basis for nearly all forms of spectroscopy. Except for differing physical constants, both involve the same “transition moment integral” or “matrix element for the transition” (21).

The electric dipole transitions are subject to several selection rules. One is the multiplicity rule.  $\Delta S = 0$  forbids transitions in which there is a change in the total electron spin quantum  $S$ . The ground state of an aromatic hydrocarbon is a singlet state ( $S = 0$ ). Half of the excited  $\pi$  electronic states are singlet states ( $S = 0$ ) and half are triplet states ( $S = 1$ ). If the triplet states were pure then only half of the excited  $\pi$  electronic states, those with  $S = 0$ , could be observed in absorption from the ground state (21).

Another is the parity selection rule in centrosymmetric molecules.  $g \leftrightarrow u$ ;  $g \leftrightarrow g$ ;  $u \leftrightarrow u$  forbids transitions between states of the same parity. The ground state of an aromatic hydrocarbon is of even ( $g$ ) parity. Half of the excited  $\pi$  electronic states are of odd ( $u$ ) parity, and half are of even ( $g$ ) parity. If the excited states were of pure multiplicity and of pure parity, then only a quarter of the excited  $\pi$  electronic states, the singlet states of odd parity, could be observed by absorption transitions from the ground state (21).

There is some relaxation of the multiplicity selection rule due to spin-orbit coupling, which introduces a small mixture of singlet character into the triplet states and

a small mixture of triplet character into the singlet states. There is some relaxation of the parity selection rule in that non-totally-symmetric vibrations distort the symmetry of the electronic state, thus introducing an admixture of opposite parity. Despite these perturbations, the selection rules limit the excited electronic states that can be observed by normal absorption spectrometry (21).

Among the large number of known organic compounds, only a small fraction displays fluorescence due to strong coupling between ground and excited states. Therefore, the fact that a molecule fluoresces can provide information regarding its structural features (17). Certain structural factors influence fluorescence. As stated previously, fluorescence is expected in molecules that are aromatic, containing conjugated double bonds with resonance stability and delocalized  $\pi$  electrons that can be placed in low-lying excited singlet states. Polycyclic aromatic systems and their derivatives with a greater number of  $\pi$  electrons than benzene will be much more fluorescent than benzene. The substituents of the aromatic ring also strongly affect fluorescence. Substituents that delocalize the  $\pi$  electrons, such as  $-\text{NH}_2$ ,  $-\text{OH}$ ,  $-\text{OCH}_3$ ,  $-\text{NHCH}_3$ , and  $-\text{N}(\text{CH}_3)_2$  groups often enhance fluorescence because they tend to increase the "transition probability" between the lowest excited singlet state and the ground state. Electron-withdrawing groups such as  $-\text{Cl}$ ,  $-\text{Br}$ ,  $-\text{I}$ ,  $-\text{NHOCH}_3$ ,  $-\text{NO}_2$ , or  $-\text{COOH}$  decrease or quench the fluorescence completely (16). Hydrogenation can also affect fluorescence. Partial hydrogenation at the site that reduces the number of rings in conjugation of aromatic molecules can cause a shift of the emission to the blue or ultraviolet region of the spectra (18).

It is generally found that the most intensely fluorescent aromatic molecules are characterized by rigid, planar structures (17). Molecular rigidity reduces the interaction of a molecule with its medium and thus reduces the rate of collisional deactivation. This reduced rate of deactivation by nonradiative processes leads to a greater probability of fluorescence (16). The principal effect of increasing molecular rigidity is to decrease vibrational amplitudes, which in turn usually reduces the efficiency of intersystem crossing and internal conversion which compete with fluorescence (17). Given a series of aromatic compounds, those that are the most planar, rigid, and sterically uncrowded are typically the most fluorescent. The probability of intermolecular energy transfer between the fluorescer and other molecules tends to be reduced at low temperature and in a medium of high viscosity in which the rotational relaxation time of the fluorescer is much longer than the lifetime of the excited state (16).

Not only is fluorescence dependent upon the structure of the molecule but also upon the environment in which the spectrum is measured. Fluorescence intensity and wavelength often vary with the solvent. Solvents capable of exhibiting strong van der Waals binding forces with the excited state species prolong the lifetime of a collisional encounter and favor deactivation. Solvents that have molecular substituents such as Br, I, NO<sub>2</sub>, or -N=N- groups are unappealing because the strong magnetic fields that surround their bulky atomic cores promote spin decoupling of electrons and triplet state formation, giving rise to marked fluorescence quenching (16). The fluorescent spectra can be shifted depending on the specific nature of the solute-solvent interactions. There are several types of generalized electrostatic solvent effects. They are (17) :

- Dipole-dipole interactions between a polar solute and a polar solvent.

- Interactions between a polar solute's permanent dipoles and induced dipoles in the solvent.
- Interactions between a polar solvent's permanent dipoles and induced dipoles in the solute.
- Dispersive interactions between the transition dipole of the solute and the induced dipole in the solvent.
- Specific short interactions such as hydrogen bonding.

In the case in which both solute and solvent possess a permanent dipole, the dipole-dipole interactions will be the predominant factors in determining magnitudes of solvent shifts in absorption and emission maxima. In most polar aromatic molecules whose lowest singlet states are  $\pi$  bonding and antibonding the excited state is more polar than the ground state. Therefore, any increase in the polarity of the solvent will produce a relatively greater stabilization of the excited than the ground state. As solvent polarity increases, the absorption and fluorescence spectra will both shift to lower energies. If both are not polar, a shift occurs because of dispersive interactions due to the fact that electronic transitions produce changes in electron density (17).

Changes in pH may also influence the fluorescence of an organic, aromatic molecule containing an acidic or basic functional group. Increasing or decreasing the pH may cause a fluorescent molecule to become nonfluorescent. This is explained by comparing the resonance forms of the anions and cations. For example, aniline in acid solution has a positive charge fixed on the nitrogen atom and the resonance forms are the same as for benzene, which fluoresces only in the ultraviolet region. However, in basic or neutral solutions, aniline has three more additional resonance structures, resulting in a



more stable excited singlet state and a longer wavelength of fluorescent radiation. Some substances are so sensitive to pH that they are used as indicators in acid-base titrations. Also the formation of chelates with metal ions promotes fluorescence by promoting rigidity and minimizing internal vibrations (16).

The quantitative relationship between the fluorescent power and concentration can also be studied. The fluorescent power is proportional to the number of molecules in excited states, which, in turn, is proportional to the radiant power absorbed by the sample. A plot of fluorescence versus concentration, shown in Figure 17, is often found to be linear over two or more decades, but there are limiting factors such as quenching and absorbance of exciting radiation by the solvent or by too high concentrations of solute (16).

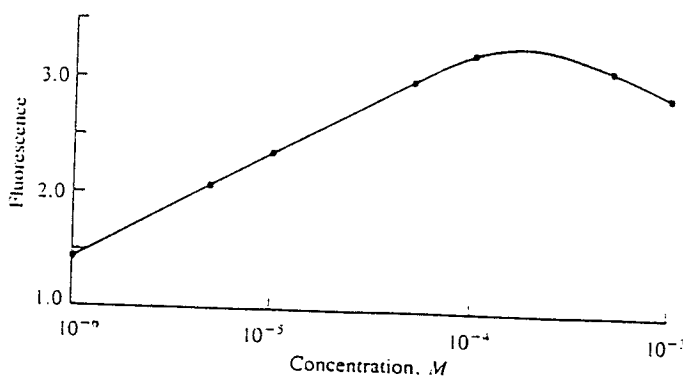


Figure 17. Fluorescence/concentration graph for the coenzyme NADH in distilled water solution. The linear portion of the curve extends from about  $10^{-4}$  to  $10^{-6}$  M. This figure was obtained from reference 16.

At high concentrations, self-quenching and self-absorption may be responsible for the negative deviations. Self-quenching results when fluorescing molecules collide and lose their excitation energy by radiationless transfer. A form of self-quenching is a

phenomenon that occurs with some solutes at high concentrations forming a complex between the excited state solute molecule and another solute molecule in the ground state. This complex is called an excimer. The excimer may then dissociate into two ground-state molecules with emission of fluorescent radiation but at longer wavelengths than the normal fluorescence. Dilution helps reduce this effect, since excimer concentration varies as the square of the solute concentration (16).

Energy transfer quenching occurs when an impurity is present whose first excited singlet state is at an energy less than that of the excited singlet state of the analytical species. Collisional impurity quenching leads to loss of fluorescence because an excited complex forms between the excited analytical species and a ground-state impurity molecule and there is subsequent nonradiative energy loss. Aromatic substances are prime offenders in this category so “spec-pure” solvents are essential (16).

Since oxygen is paramagnetic, one of the most troublesome limiting factors of fluorescence is the ability of molecular dissolved oxygen to quench excited singlet and triplet states of many molecules, especially aromatic hydrocarbons, in solution. Just about all collisions between oxygen molecules and excited hydrocarbons are effective (17). Therefore, oxygen must be removed from solutions by degassing with nitrogen or other inert gases before fluorescence measurements are made (16).

Specifically examining 9-anthryldiazomethane (ADAM), one can see why it is so strongly fluorescent. ADAM contains an anthryl group which is a complex hydrocarbon consisting of three fused rings. This structure is highly conjugated with resonance stability. It is rigid, planar, and the  $\pi$  electrons are delocalized. The substituent on the anthryl group of ADAM is  $\text{CHN}_2$ . It acts as an electron donor that stabilizes and may

enhance the fluorescence. The same is true for the proposed derivative in which the substituent on the anthryl ring is a phosphoester. Since ADAM contains polar groups, when it is in a polar environment there will be a greater stabilization of the excited state due to dipole-dipole interactions. ADAM and the proposed derivative can undergo hydrogen bonding with the solvent which will also stabilize fluorescence. The pH of the solution does not seem to alter the electron donating ability and, therefore, does not affect the fluorescence. Since ADAM has the fundamental characteristics of a good fluorescer, it is expected to be useful as a highly fluorescent label for nucleotides.

## Chapter 3

### Experimental

The experimental work will be presented in four parts as follows:

Part A: Experiments with purchased ADAM

Part B: Synthesis of ADAM

Part C: Purification of ADAM

Part D: Experiments with synthesized ADAM

In part A, ADAM was purchased from Kamiya Biomedical Company and reacted with adenine-5'-monophosphate (AMP) and other phosphorylated compounds in numerous solvents and conditions. Part B provides the details for synthesizing ADAM by three different methods. Various purification techniques were performed on the synthesized ADAM in order to remove impurities and hydrolysed products (part C). Finally, in part D, the synthesized ADAM was reacted with the sodium salt and acidic form of AMP in several solvents and conditions.

#### **Part A: Experiments with Purchased ADAM**

**Materials:** 9-anthryldiazomethane (ADAM) was purchased from Kamiya Biomedical Company, Seattle, WA. Adenine 5'-monophosphate sodium salt (AMP), fructose-1,6-diphosphate, and cytidine 5'-triphosphate (CTP) were purchased from Sigma Chemical Company, St. Louis MO. Acetone, methanol, cellulose plates, and silica gel mesh 60 Å were purchased from Aldrich Chemical Company, Milwaukee, WI. Ether, hydrochloric acid, formic acid, sulfuric acid, glacial acetic acid, acetonitrile, and methylene chloride were purchased from Fisher Scientific, Fairlawn, NJ. Isopropanol, ammonium

molybdate, aluminum chloride hexahydrate, and potassium dihydrogen phosphate monohydrate were obtained from J. T. Baker Chemical Company, Phillipsburg, NJ. Sodium hydroxide and sodium chloride were purchased from VWR Scientific, West Chester, PA. Stearic acid and sodium acetate were obtained from Mallinckrodt, St. Louis, MO. The aluminum backed silica thin layer chromatography (TLC) plates with and without fluorescent indicator were purchased from Whatman, Kent, England and the reverse phase silica TLC plates were purchased from Analtech, Newark, DE. All materials were reagent grade and used without further purification.

Instrumentation: High pressure liquid chromatography (HPLC) analysis was performed on an IBM LC/9533 Ternary gradient with a reverse phase C18 Rainin analytical column (4.6 x 250 mm) and a ultraviolet (UV) detector set at 256 nm. The ultraviolet lamp that was used to detect fluorescence on the TLC plates was purchased from UVP. The UV spectral data were obtained using a Hewlett Packard diode array spectrophotometer model 8452 A. Nuclear magnetic resonance (NMR) spectra were recorded with a Gemini 2000 Varian 400 MHz analyzer. Gas chromatography/mass spectrometry (GC/MS) data were obtained on a Finnigan GCQ.

#### 1. ADAM and AMP (Sodium Salt)

Adenine 5'-monophosphate (AMP) was chosen as the nucleotide in initial attempts of labeling with 9-anthryldiazomethane (ADAM). Many reaction conditions were explored such as variations in solvents, temperatures, pHs, concentrations, and acidic additives (Table 1). Reactions were also conducted under fluorescent or UV light as well as in the dark. AMP was dissolved in deionized water or methanol at

concentrations of 0.1 mg/mL and 0.7 mg/mL. Aqueous AMP was adjusted with HCl or NaOH to a variety of pHs (3, 4, 5, 6, 7, 8.5, and 10.5). ADAM : AMP molar ratios were varied at 100:1, 10:1, and 1:1. In several different combinations of solvents, the reactions took place in microliter amounts of 500  $\mu$ L or less in the dark or under UV light and at room temperature (RT) or 30°C. Several acids were used to acidify the reaction mixture such as silica gel, HCl, 0.2 mM formic acid in methanol, sulfuric acid, glacial acetic acid and the Lewis acid aluminum chloride ( $\text{AlCl}_3$ ). All reactions were run along with the appropriate control reactions. Reactions were monitored by TLC using cellulose plates developed in 100 % 0.15 M NaCl and 80:20 (v/v) 0.15 M NaCl : acetonitrile. Reverse phase silica plates were developed in 50:50 (v/v) 10 mM sodium acetate (pH 6) : acetonitrile or 50:50 (v/v) water : acetonitrile. Silica plates were developed in the following solvents: 15:85 (v/v), 20:80 (v/v), 25:75 (v/v), 5:95 (v/v) MeOH : methylene chloride as well as 20:80 (v/v) MeOH : ether. ADAM and derivatives were detected on the TLC plate by UV at 254 nm and AMP was detected on the TLC plate with ammonium molybdate (0.4 g in 20 mL of 5 %  $\text{HNO}_3$ ). The diode array spectrophotometer was used to measure the absorbance of ADAM, AMP, and the reaction mixture at 256, 260, and 280 nm. GC/MS and  $^{31}\text{P}$  NMR was run on an unidentified product. HPLC with a mobile phase of 50:50 (v/v) acetonitrile : water and 100 % acetonitrile was also used to detect ADAM and derivative in the reaction mixture.

## 2. ADAM and other Phosphorylated Compounds

Potassium dihydrogen phosphate ( $\text{KH}_2\text{PO}_4$ ) was used as a model compound in the reaction with ADAM. 20  $\mu$ L of  $\text{KH}_2\text{PO}_4$  (8 mg/100 mL water) was mixed with 200  $\mu$ L of ADAM at a 100 fold molar excess. All reactions were conducted at room temperature

and either in the dark or under a UV lamp at 254 nm. TLC was performed on reverse phase silica plate using 50:50 (v/v) 10 mM sodium acetate (pH 6) : acetonitrile.

25  $\mu$ L of fructose-1,6-diphosphate, 0.8 mg/mL, was reacted with 25  $\mu$ L of ADAM at 0.05 % (w/v) in the dark at room temperature. The reaction was monitored by TLC on reverse phase silica plates developed in 50:50 (v/v) and 95:5 (v/v) acetonitrile : water or 20:80 (v/v) MeOH : ether was used. The ADAM and reaction mixture were injected into the HPLC with a mobile phase of 50:50 (v/v) acetonitrile : water or 100 % acetonitrile.

200  $\mu$ L of cytidine 5'-triphosphate (CTP) at 1 mg/mL was reacted with 200  $\mu$ L of ADAM at 0.8 mg/mL at room temperature in the dark. TLC was done on reverse phase silica plates using 50:50 (v/v) acetonitrile : water as the mobile phase.

### 3. ADAM and Stearic acid

As a check on the quality of the purchased ADAM, stearic acid, an eighteen carbon saturated fatty acid, was reacted with ADAM. Two different literature procedures were followed. The first used 40  $\mu$ L of stearic acid at 3mg/mL in ether mixed with 400  $\mu$ L of ADAM at 2mg/mL in ether (100 fold molar excess). The reaction was performed in the dark at room temperature. In the second procedure 25  $\mu$ L of ADAM at 0.05 % (0.7 mg/mL) in methanol was mixed with 25  $\mu$ L of stearic acid at the same concentration as above. The reactions were monitored by TLC on reverse phase silica plates developed in 50:50 (v/v) acetonitrile : water.

Table 1. Summary of Reactions and Conditions

<u>Solvent</u>		<u>Conditions</u>
<u>ADAM</u>	<u>AMP</u>	
Acetone	Water	0.1 % (w/v) ADAM. pH 3, 4, 5, 6, 7, 8.5, 10.5. RT. Silica gel, formic acid.
Acetone	Water/isopropanol 1:10 (v/v)	0.2 % (w/v) ADAM, HCl, RT.
MeOH	MeOH	Silica gel (30°C), sulfuric acid (UV, 30°C), HCl, formic acid, acetic acid, no additives. 1:1 and 1:10 molar ratio AMP : ADAM. 0.05% (w/v) and 0.2% (w/v) ADAM.
MeOH	Water	AlCl <sub>3</sub> , RT.
Acetone	MeOH	No additives, HCl, silica gel, 30°C.
Ether	MeOH	No additives, formic acid, acetic acid, silica gel, ADAM at 0.2 % (w/v) and 0.05 % (w/v).
<u>ADAM</u>	<u>KH<sub>2</sub>PO<sub>4</sub></u>	
MeOH	Water	pH 6 in the dark, pH 3 under UV, pH 2 in the dark, pH 6 under UV. All at RT.
<u>ADAM</u>	<u>Fruc-1,6-diphos.</u>	
MeOH	Water	0.05% (w/v) ADAM, RT.
<u>ADAM</u>	<u>CTP</u>	
MeOH	Water	RT.



<u>ADAM</u>	<u>Stearic Acid</u>	
Ether	Ether	RT, 100 molar excess ADAM.
MeOH	Ether	0.05% (w/v) ADAM, RT.

### **Part B: Synthesis of ADAM**

**Materials:** Potassium permanganate was purchased from J. T. Baker Chemical Company, Phillipsburg, NJ. Activated carbon, 9-anthraldehyde, quinuclidine, N-chlorosuccinimide (NCS), and 55 % hydrazine hydrate were purchased from Aldrich Chemical Company, Milwaukee, WI. Absolute ethanol was purchased from Quantum, Tuscola, IL. Ethyl acetate, glacial acetic acid, ether, and hexane were purchased from Fisher Scientific, Fairlawn, NJ. Yellow mercuric oxide was obtained from Allied Chemical, Morristown, NJ. Anhydrous sodium sulfate was purchased from Matheson Coleman and Bell, Norwood, OH. Potassium hydroxide was purchased from VWR Scientific, West Chester, PA. The aluminum backed silica TLC plates with fluorescent indicator were purchased from Whatman, Kent, England and the reverse phase silica TLC plates were purchased from Analtech, Newark, DE. All materials were reagent grade and used without further purification.

**Instrumentation:** All melting points were obtained from Mel-Temp Laboratory Devices. The ultraviolet lamp that was used to detect fluorescence on the TLC plates was purchased from UVP. The rotovap used was a Buchi Rotovapor (R-114). Infrared (IR) spectra were obtained from a Perkin-Elmer 1600 Series FTIR.

#### 1. Preparation of ADAM using manganese dioxide

a. Preparation of activated manganese dioxide (24 and 25)

A solution of 2 g potassium permanganate in 25 mL water was stirred at room temperature with 1 g activated carbon for 20 hours. The suspension was filtered and washed with deionized water in a Buchner funnel and then oven dried at 100 °C for 24 hours.

b. Preparation of 9-anthraldehyde hydrazone (6)

A solution of 8.8 g 9-anthraldehyde in 150 mL absolute ethanol was stirred with 12 mL of 55 % hydrazine hydrate at room temperature for 3 hours. The resulting product was vacuum filtered and oven dried. The solid was recrystallized in absolute ethanol. The melting point was 119-120 °C; literature value is 124-126°C.

c. Preparation of ADAM (11)

0.2 g 9-anthraldehyde hydrazone, prepared as in B1b above, was dissolved in 100 mL anhydrous ether. 0.8 g activated manganese dioxide was added and the solution was stirred vigorously for 15 minutes. The reaction was stopped by filtering off the manganese dioxide. The orange-red ether solution was rotovapped and stored at -20 °C. An IR spectrum gave a diazo band at 2100  $\text{cm}^{-1}$ . The melting point was 55-60 °C; literature value is 63-64 °C. TLC was done on reverse phase plates developed in 50:50 (v/v) acetonitrile : water, and on silica plates using 50:50 (v/v) hexane : ethyl acetate and 100 % hexane as the mobile phase. Detection was with UV light.

2. Preparation of ADAM using mercuric oxide (6)

1 g 9-anthraldehyde hydrazone, prepared as in B1b above, in 12.5 mL ether was stirred with 2.5 g yellow mercuric oxide, 1 g anhydrous sodium sulfate, and 0.25 mL KOH saturated ethanol for five hours at room temperature. The bright red solution was

filtered, rotovapped and stored at  $-20\text{ }^{\circ}\text{C}$ . The melting point was  $48\text{--}62\text{ }^{\circ}\text{C}$ ; literature value is  $63\text{--}64\text{ }^{\circ}\text{C}$ . An IR spectrum gave a diazo band at  $2060\text{ cm}^{-1}$ . A few drops of glacial acetic acid was added to a small piece of solid ADAM. The acid reacted violently and exothermically with the solid. TLC of ADAM was performed on silica plates in 50:50 (v/v) hexane : ethyl acetate and detected with UV light.

### 3. Preparation of ADAM using N-chlorosuccinimide (NCS) (26)

To  $500\text{ }\mu\text{L}$  of  $6.9\text{ mmol/L}$  9-anthraldehyde hydrazone, prepared as in B1b above, in ethyl acetate was added  $500\text{ }\mu\text{L}$  of  $69.0\text{ mmol/L}$  quinuclidine solution in ethyl acetate and  $500\text{ }\mu\text{L}$  of  $6.9\text{ mmol/L}$  NCS in ethyl acetate and the solution was mixed. The mixture was allowed to stand at room temperature for 30 minutes and then used directly. TLC was performed on silica plates in 3:2 hexane : ethyl acetate. IR spectra gave a diazo band at  $2084\text{ cm}^{-1}$ .

## **Part C: Purification of Crude ADAM**

**Materials:** 9-anthryldiazomethane was prepared according to B2 above. 9-anthraldehyde hydrazone was prepared according to B1b. Carbon tetrachloride, petroleum ether, florisil 60–100 mesh, hexane, ethyl acetate, HPLC grade acetonitrile, and neutral alumina were purchased from Fisher Scientific, Fairlawn, NJ. Triethylamine was purchased from J. T. Baker chemical Company, Phillipsburg, NJ. Methanol, acetone, silica gel mesh  $60\text{ }\text{\AA}$ , and calcium carbonate were purchased from Aldrich Chemical Company, Milwaukee, WI. The florisil plates were purchased from Analtech, Newark, DE. The aluminum backed silica TLC plates with fluorescent indicator were purchased from Whatman, Kent, England and the reverse phase silica TLC plates were purchased from Analtech, Newark,

Delaware. The argon gas was purchased from Praxair. All materials were reagent grade and used without further purification.

Instrumentation: The ultraviolet lamp that was used to detect fluorescence on the TLC plates was purchased from UVP, San Gabriel, CA. The IR spectra were obtained from a Perkin-Elmer 1600 Series FTIR. HPLC analysis was performed on an IBM LC/9533 Ternary gradient with a reverse phase C18 Rainin analytical column (4.6 x 250 mm) and a ultraviolet (UV) detector set at 256 nm.

### 1. Gravity Column

3.4 g florisil was prepared as a wet slurry in 50:50 (v/v) hexane : ethylacetate in a 0.5 x 20 cm column. 0.06 g ADAM was dissolved in ethylacetate. 100 mL of 50:50 (v/v) hexane : ethyl acetate was used as the mobile phase. TLC was done on every third collected fraction on florisil plates in 50:50 (v/v) hexane : ethyl acetate and detected with UV light. IR spectra were obtained on several fractions.

### 2. Flash Columns

#### a. Florisil

7.85 g florisil was dry packed in a 1 x 45 cm column and wet with hexane. The mobile phase consisted of several solvents including a gradient of hexane and ethyl acetate and argon gas. 0.0625 g of the crude ADAM was dissolved in ethyl acetate and was eluted through the column with 80 ml of each of the following solvents beginning with 100 % hexane, then 75:25 (v/v), 50:50 (v/v), 25:75 (v/v), 0:100 (v/v) hexane : ethyl acetate, 100 % acetone, and concluding with 100 % methanol. TLC was performed on florisil plates in 50:50 ethyl acetate : hexane on every third fraction collected and

detected with UV light. Also, the reverse polarity order of the solvents was used, 100 % methanol, 50:50 ethyl acetate : hexane, and 100 % hexane.

b. Silica

Several solvent systems were used with a silica column. In each case, 8 g of silica was dry packed in a 1 x 45 cm column and wet with hexane. 0.1 g of crude ADAM was dissolved in 1 mL ethyl acetate, placed on the column, and eluted with 80 ml of the solvents making up the mobile phase in the order listed below.

- 100:0 (v/v), 80:20 (v/v), 60:40 (v/v), 40:60 (v/v), 20:80 (v/v), 0:100 (v/v) hexane : ethyl acetate, 100 % methanol, 100 % acetone
- 1 % (v/v) triethylamine in hexane as column pretreatment and then the solvents as above
- using acetonitrile before acetone in the order above

Also, 0.10 g ADAM was dissolved in 0.5 mL  $\text{CCl}_4$  and a silica column with mobile phase 10 % water in petroleum ether/ $\text{CCl}_4$  was used.

All TLCs were done on silica plates with fluorescent indicator in 3:2 (v/v) hexane : ethyl acetate and detected with UV light.

c. Calcium carbonate

6.0 g calcium carbonate was dry packed in a 1 x 45 cm column and wet with hexane. 0.1 g of crude ADAM was dissolved in 1 mL ethyl acetate, applied to the column, and eluted with 80 ml of the mobile phase which consisted of a hexane and ethyl acetate gradient. The order was 100:0 (v/v), 75:25 (v/v), 50:50 (v/v), 100:0 (v/v) hexane: ethyl acetate. TLCs were performed on silica plates with indicator in 3:2 (v/v) hexane : ethyl acetate and detected with UV light.

#### d. Alumina

13 g of alumina was dry packed in a 1 x 45 cm column and wet with  $\text{CCl}_4$ . 0.1 g ADAM was dissolved in  $\text{CCl}_4$  and eluted through the column with 80 ml of each of the solvents in the mobile phase. The mobile phase was 100 %  $\text{CCl}_4$ , 75:25 (v/v)  $\text{CCl}_4$  : methanol, and 100 % methanol. TLCs on every third fraction were done on reverse phase silica plates in 100 % acetonitrile and detected with UV light. A second solvent system using  $\text{CCl}_4$ , followed by ethyl acetate, and then acetone was employed. TLC was done on silica developed in 3:2 (v/v) hexane : ethyl acetate. Finally, ADAM was dissolved in hexane and the mobile phase was hexane, followed by  $\text{CCl}_4$ , then ethyl acetate, and finally acetone.

#### 3. Sublimation

Vacuum sublimation was performed in a Chemglass piece (model # CG-3038-01) at room temperature with a dry ice-acetone coldfinger and a schlink line. Also, tube sublimation was set up at 50 °C and water-cooled. Both sublimations proceeded for three days.

#### 4. HPLC

0.0082 g/mL 9-anthraldehyde, 0.0018 g/mL 9-anthraldehyde hydrazone, and 0.0110 g/mL ADAM were dissolved in HPLC grade acetonitrile and injected (10  $\mu\text{L}$ ) into the HPLC with 100 % acetonitrile as the mobile phase. The flow rate was 0.4 or 1.0 mL/min and the UV detector was set at 256 nm. The crude ADAM gave seven peaks that were collected individually, rotovapped, and stored at -20 °C.

**Part D: Experiments with Synthesized ADAM**

**Materials:** 18-crown-6, methanol, silica gel mesh 60 Å, 1,3-dimethyl-oxo-hexahydro-pyrimidine (DMPU), and pyridine were purchased from Aldrich Chemical Company. AMP (acidic), AMP (sodium salt), CTP, were purchased from Sigma Chemical Company, St. Louis, MO. Tetrahydrofuran (THF) was purchased from Sargent-Welch, Stokie, IL. Chloroform and sodium hydroxide were purchased from VWR Scientific, West Chester, PA. Stearic acid was purchased from Mallinckrodt, St. Louis, MO. Ether, acetonitrile, hydrochloric acid, methylene chloride, hexane, and ethyl acetate were purchased from Fisher Scientific, Fairlawn, NJ. Silica plates were purchased from Whatman, Kent, England. ADAM was prepared according to B2 described previously. All chemicals were reagent grade and used without further purification.

**Instrumentation:** The ultraviolet lamp that was used to detect fluorescence on the TLC plates was purchased from UVP.

All reactions were monitored by TLC on silica plates with fluorescent indicator developed in 3:2 (v/v) hexane : ethyl acetate and detected under UV light. ADAM's spots were fluorescent under UV light and AMP and stearic acid appeared dark against a fluorescent background. Unless otherwise noted, all of the reactions occurred at room temperature in the dark for 24 hours. The appropriate controls were used for each experiment.

1. Reactions with ADAM prepared as in B2
  - a. ADAM and Stearic acid

- 40  $\mu\text{L}$  of 2.8 mg/mL stearic acid in ether ( $9.55 \times 10^{-6}$  mol) and 400  $\mu\text{L}$  of 2.0 mg/mL ADAM in ether ( $1 \times 10^{-4}$  mol) were mixed.
- Rotovapped HPLC fractions were dissolved in 1 mL of ether. 100  $\mu\text{L}$  of each were reacted with 10  $\mu\text{L}$  of 2.8 mg/mL stearic acid in ether.

b. ADAM and AMP (Sodium Salt)

- 40  $\mu\text{L}$  of 3.5 mg/mL AMP in methanol ( $1 \times 10^{-5}$  mol) and 400  $\mu\text{L}$  of 2.1 mg/mL ADAM in methanol ( $1 \times 10^{-4}$  mol) were mixed.
- 40  $\mu\text{L}$  of 1.6 mg/mL AMP in  $4.5 \times 10^{-6}$  M HCl and 400  $\mu\text{L}$  of 0.01 g/mL ADAM in methanol were mixed.
- 40  $\mu\text{L}$  of 1.6 mg/mL AMP in  $4.5 \times 10^{-6}$  M HCl and 400  $\mu\text{L}$  of 1.3 mg/mL ADAM in acetonitrile were mixed.
- 40  $\mu\text{L}$  of 3.5 mg/mL AMP in 10 % pyridine-HCl in deionized water and 400  $\mu\text{L}$  of 2 mg/mL ADAM in methanol were mixed and placed in a cold room.
- 40  $\mu\text{L}$  of 3.5 mg/mL AMP in methanol ( $1 \times 10^{-5}$  mol), 400  $\mu\text{L}$  of 2.1 mg/mL ADAM in methanol ( $1 \times 10^{-4}$  mol), and 80  $\mu\text{L}$  of 5 % 18-crown-6 (0.05 g/mL) were mixed.
- 40  $\mu\text{L}$  of 3.5 mg/mL AMP in 10 % (w/v) 18-crown-6 in methanol, 400  $\mu\text{L}$  of 2.1 mg/mL ADAM in methanol, and 0.02 g silica gel were mixed.
- 5 % 18-crown-6 (0.116 g) and 0.03 g ADAM were dissolved in 2 mL of each of the following: THF, methylene chloride, DMPU, and chloroform. 1.5 mg AMP was dissolved in 1 mL 10 % (v/v) pyridine-HCl (deionized water). 500  $\mu\text{L}$  of each of the organic solutions were vigorously stirred with 500  $\mu\text{L}$  of the AMP solution at 37 °C, in a cold room, and at room temperature.



c. ADAM and AMP (Acidic)

- 80  $\mu\text{L}$  of 4 mg/mL AMP in ether or water were each stirred with 800  $\mu\text{L}$  of 2 mg/mL ADAM in ether in a cold room. Also, the same concentrations of AMP and ADAM dissolved in methanol was explored.
- 800  $\mu\text{L}$  of 45 mg/mL ADAM in methanol was stirred vigorously with 80  $\mu\text{L}$  of 3.5 mg/mL AMP methanol in a cold room.
- 500  $\mu\text{L}$  of 4 mg/mL ADAM in methanol was reacted with 50  $\mu\text{L}$  of 3 mg/mL AMP in water (NaOH) at pH 7, 9, and 12.
- 1 mL of 2 mg/mL ADAM in DMPU was stirred vigorously with 0.5 mL of 3.5 mg/mL AMP in three different solvents, deionized water, methanol, and DMPU.

d. ADAM and CTP

- 200  $\mu\text{L}$  of 2 mg/mL CTP in deionized water was mixed with 200  $\mu\text{L}$  of 5 mg/mL ADAM in acetonitrile.

2. Reactions with ADAM prepared as in B3

a. ADAM and Stearic Acid

- 400  $\mu\text{L}$  of ADAM and 40  $\mu\text{L}$  of 2.8 mg/mL stearic acid in ether were mixed.

b. ADAM and AMP (Sodium Salt)

- 500  $\mu\text{L}$  of ADAM was stirred with 500  $\mu\text{L}$  of 1.5 mg/mL AMP in deionized 10 % (v/v) pyridine-HCl (v/v) in a cold room for 24 hours.

c. ADAM and AMP (Acidic)

- 500  $\mu\text{L}$  of ADAM was stirred with 500  $\mu\text{L}$  of 1.5 mg/mL AMP in deionized water in a cold room for 24 hours.

## Chapter 4

### Results and Discussion

9-anthryldiazomethane (ADAM) was first developed as a fluorescent labeling reagent for fatty acids (11). ADAM forms an ester bond with carboxyl groups and, in this respect, reacts like diazomethane. ADAM was later used to fluorescently label amino acids (12) and N-acetylamino acids (13) *via* ester bond formation.

A search of the literature revealed that diazomethane has been used to methylate phosphonic acids (14). Since ADAM reacts like diazomethane, it seemed reasonable to assume that ADAM should also be able to derivatize phosphonic acids. Furthermore, it seemed reasonable to assume that ADAM could be used in the making of phosphoric acid esters.

Many biological molecules are phosphorylated. We wished to extend ADAM's use as a fluorescent labeling reagent to include phosphorylated as well as carboxyl containing biomolecules. Our goal was to find suitable conditions of solvent, reactant concentrations, and temperature which would lead to the rapid derivatization of phosphorylated biomolecules. Ideally, this would be achieved simply by mixing ADAM with the desired compound.

A number of model compounds were used including fructose-1,6-diphosphate, potassium dihydrogen phosphate, cytidine-5'-triphosphate, and primarily adenosine-5'-monophosphate (AMP). Figure 18 gives the proposed reaction of ADAM and AMP. A wide variety of techniques were used in this project. TLC was used to monitor the products of the reactions which were detected by UV. IR was used to detect the diazo found in the synthesized ADAM. Attempts to separate the mixture after synthesis of the

crude ADAM mixture utilized gravity, flash, and high pressure liquid chromatography. Mass spectrometry and  $^{31}\text{P}$  NMR were used to search for the presence of an ADAM-AMP derivative. A fuller discussion of the results follows in four parts.

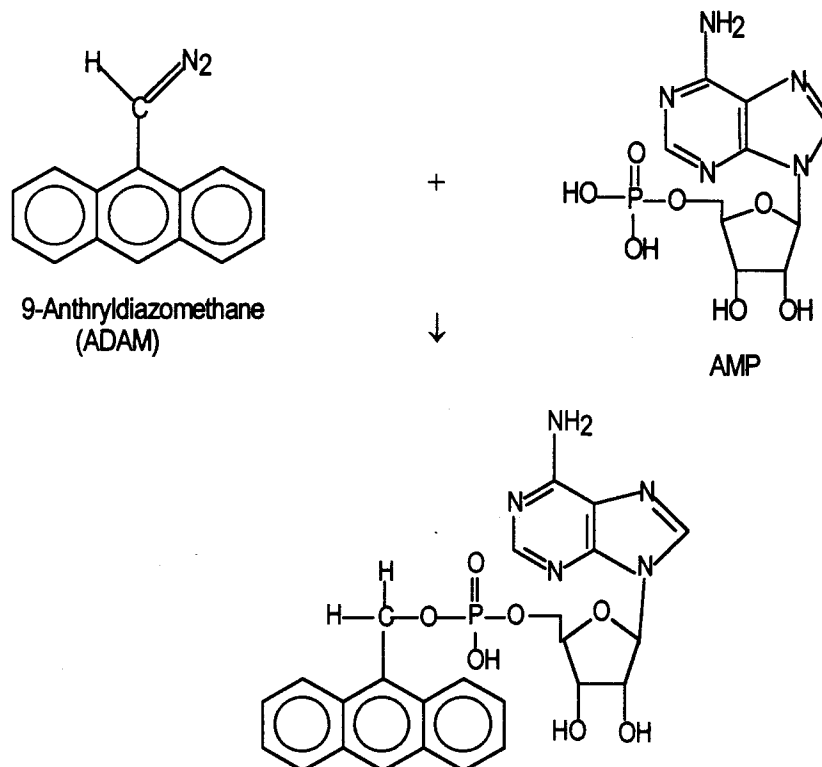


Figure 18. Proposed reaction of ADAM with AMP

### Part A: Experiments with Purchased ADAM

The purchased ADAM gave four to six spots on the TLC plates. Kamiya Biomedical Company explained in a letter that ADAM was very unstable and contained many impurities, only being about 20 % pure. They stated that this should not affect its usefulness in labeling fatty acids.

The first step in the proposed reaction mechanism for ADAM and AMP is that a proton is extracted from the phosphate group of AMP, and the second step is that the

negatively charged phosphate group acts as a nucleophile. Hence, the pH of the reaction mixtures of ADAM and AMP were varied from a low pH to protonate the phosphate group on AMP to a moderately high pH to stabilize the negative charge on the phosphate group of AMP. When 200  $\mu\text{L}$  of 0.7 mg/mL AMP was dissolved in water at pH 6 and reacted with 200  $\mu\text{L}$  of 0.6 mg/mL ADAM in methanol, an extra spot was seen on the reverse phase silica plate that did not correspond to either of the two reactants. Barker *et al.* (11), Kawakami *et al.* (13 and 23), and Yoshida *et al.* (12) used HPLC with a reverse phase column to detect their derivatives. HPLC was performed following the guidelines used by Barker and colleagues (11) on the reaction mixture and the first peak was collected. Also the TLC spot was scraped off and the spot was eluted with ether.  $^{31}\text{P}$  NMR was done on the HPLC fraction and GC/MS and MS using a solid phase probe was performed on the solution from the extra spot on the TLC plate. The initial  $^{31}\text{P}$  NMR gave three peaks at 3.769 ppm, 7.305 ppm, and 27.934 ppm which were just above the noise signals (Figure 19). After a 24 hour run, several different peaks appeared at 1.184 ppm, 3.808 ppm, and 76.953 ppm which were also slightly above the noise (Figure 20). The AMP standard showed a peak at 1.915 ppm. This peak was not apparent in the ADAM-AMP sample. The NMR spectra results were difficult to interpret due to the very low signal to noise ratio. The compound or compounds present, if any, may have been unstable and decomposed based on the 24 hour scan. The GC/MS spectra only showed peaks corresponding to silica and/or silicone. It was thought that these peaks were either due to the column itself or from the TLC plate. The mass spectra using the solid phase probe gave peaks corresponding to 9-methylanthracene with a mass peak at 192 and several small peaks signifying fragments of AMP such as a mass peak at 135. There

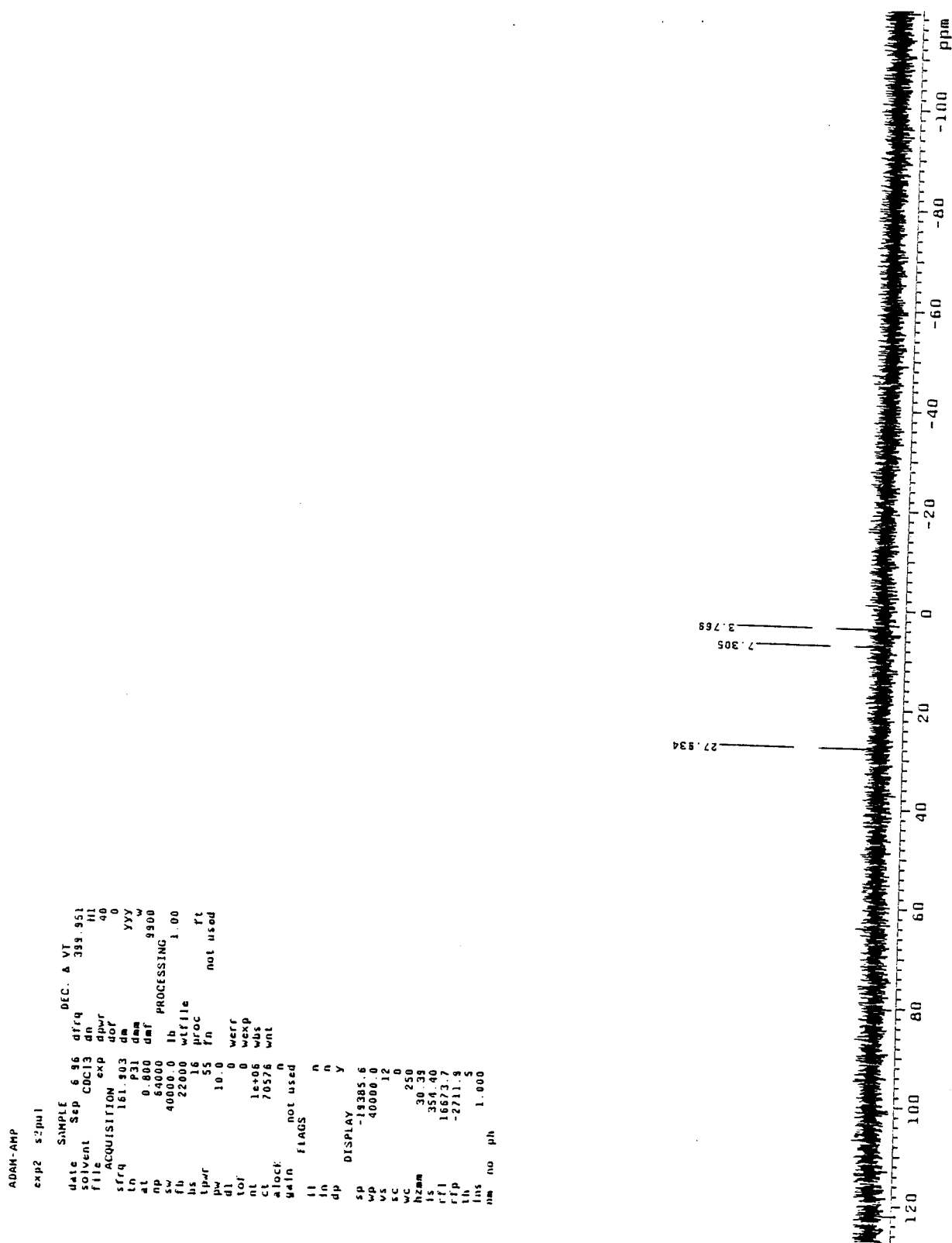
were no peaks that indicated the fragmentation of an AMP-ADAM derivative. The UV spectra from the diode array also did not provide any concrete data suggesting an ADAM-AMP derivative. AMP absorbs at 260 and 280 nm and ADAM absorbs at 256 nm.

A number of reagents were used to acidify the reaction medium. Unfortunately, some acids may have been too strong. Kawakami and colleagues (13) tried several inorganic acids and found that silica gel produced the best yields. Silica gel was used but no derivative was found based on the results from the TLC.

All other reactions with different phosphorylated compounds failed to produce a fluorescent derivative identified by TLC.

Since ADAM is known to derivatize fatty acids, stearic acid was used as a check on the purchased ADAM. A procedure given by Barker and colleagues (11) was followed but no derivative was found. The Kamiya Biomedical Company also published an insert with ADAM using a slightly different procedure of derivatizing fatty acids. This method was also used but, again, no derivatives were seen.

The main concern was the concentration of pure ADAM in the reaction mixture since stearic acid, a saturated fatty acid, did not react to produce a derivative. Another major concern was cost. After shipping and handling, it cost \$300.00 for 100 mg of ADAM. We felt that that we could synthesize it just as well and more cheaply following several articles describing the procedure.

Figure 19. Initial  $^{31}\text{P}$  NMR Spectrum of Derivative

```

9-13-96-31P ADAM-AMP
exp4 s2pu1

SAMPLE DEC. & VT
date Sep 12 96 dfrq 399.952
solvent 020 dn H1
file /usr/local/dpwr 40
1/nmrdata/Serra/AD~ dof 0
AM-AMP-P31 dm YYY
ACQUISITION dnm w
sfrq 161.903 dmf 9900
tn P31 PROCESSING
at 0.800 lb 1.00
np 64000 vtfile
sw 40000.0 proc ft
fb 22000 tn not used
bs 16
tpwr 55 werr
pw 10.0 wexp
dl 0 wbs
tof 0 wnt
nt 200000
ct 71680
alock n
gain not used

FLAGS
ll n
ln n
dp y

DISPLAY
sp -19382.9
wp 40000.0
vs 37
sc 0
wc 250
hzmm 160.00
ls 354.40
rf1 19382.9
rfp 0
th 30
lms 1.000
nm no ph

```

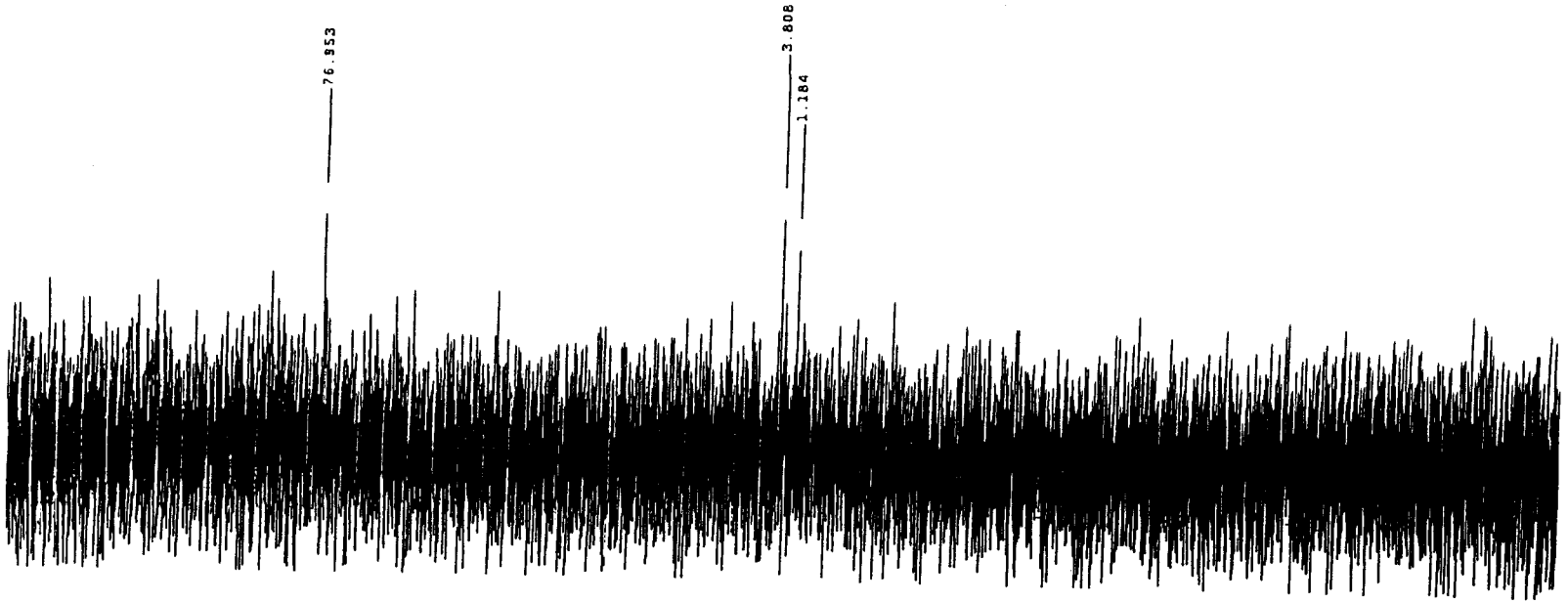


Figure 20. 24 Hour  $^{31}\text{P}$  NMR of Derivative

## Part B: Synthesis of ADAM

Since a main concern was the purity of the purchased ADAM, we decided to synthesize it following three different procedures. Barker and colleagues (11) used manganese dioxide to oxidize 9-anthraldehyde hydrazone to ADAM. They obtained a 92 % yield and saw a strong diazo band at  $2080\text{ cm}^{-1}$ . In a later paper (24), they discussed that the activated manganese dioxide used in the original work purchased from Sterling-Winthrop Chemical Company was no longer available. They used a method from Carpino (25) to synthesize activated manganese dioxide from activated carbon and potassium permanganate. However, Carpino explained that not all commercial activated carbon was satisfactory. ADAM synthesized by this procedure gave a product that had a weak IR absorbance at  $2100\text{ cm}^{-1}$  (Figure 21). TLC plates showed the presence of at least six spots indicating our yield was considerably less than 92 %. A limiting factor was thought to be producing enough of the activated manganese dioxide since the activated carbon was not sufficiently satisfactory. This method was abandoned.

Another method for synthesis of ADAM at 65 % yield was discovered by Nakaya *et al.* (6) using mercuric oxide. This procedure was used and it seemed to give a larger IR diazo band at about  $2100\text{ cm}^{-1}$  (Figure 22). However, there were still the same six spots on the TLC plate (Figure 24) as seen in the activated manganese dioxide method.

Barker *et al.* (11) demonstrated that solid ADAM reacted rapidly and exothermically with the evolution of nitrogen gas when a few drops of glacial acetic acid were added. The crude ADAM synthesized by the mercuric oxide method reacted in the same manner. This evidence coupled with the IR spectrum indicated that ADAM was present.



A third method for synthesis of ADAM using N-chlorosuccinimide (NCS) was followed according to Yoshida *et al.* (26). A diazo band was seen on the IR spectra at  $2084\text{ cm}^{-1}$  (Figure 23) and only two spots were seen on the TLC plate (Figure 24).

To attempt to identify all of the spots seen on the TLC for ADAM, the synthesized ADAM was compared to other anthracene compounds. ADAM synthesized by the mercuric oxide method dissolved in acetonitrile, as well as 9-anthraldehyde, 9-anthraldehyde hydrazone, 9-anthracene methanol (purchased from Aldrich Chemical Company), 9-methylanthracene (purchased from Aldrich Chemical Company) dissolved in ether, and ADAM synthesized by the NCS method were chromatographed by TLC on silica plates in 3:2 (v/v) hexane : ethyl acetate. The TLC is presented in Figure 24. The ADAM synthesized by the mercuric oxide method, #1 on the figure, gave six spots plus one at the origin with  $R_f$  values of 0.70, 0.58, 0.48, 0.35, 0.25, 0.14, and 0 mm. The first spot on the TLC for synthesized ADAM is thought to be either 9-anthraldehyde ( $R_f$  value of 0.69 mm) or 9-methylanthracene ( $R_f$  value of 0.70 mm). The second spot on ADAM could be 9-anthracene methanol which itself contains impurities ( $R_f$  values of 0.67, 0.56, 0.45, and 0.35 mm). The third spot for ADAM corresponds to 9-anthraldehyde hydrazone which also contains some 9-anthraldehyde ( $R_f$  values of 0.70 and 0.49 mm). ADAM synthesized by the NCS method, # 6 on the figure, only had two spots with  $R_f$  values of 0.69 and 0 mm. The spot at the sample origin seen in both methods of synthesizing ADAM is proposed to be the 9-anthryldiazomethane. In previous experiments, this spot at the origin of a silica TLC plate disappeared when glacial acetic acid was added to both of the synthesized ADAM solutions suggested by Barker *et al.*

Figure 21. IR of ADAM using manganese dioxide

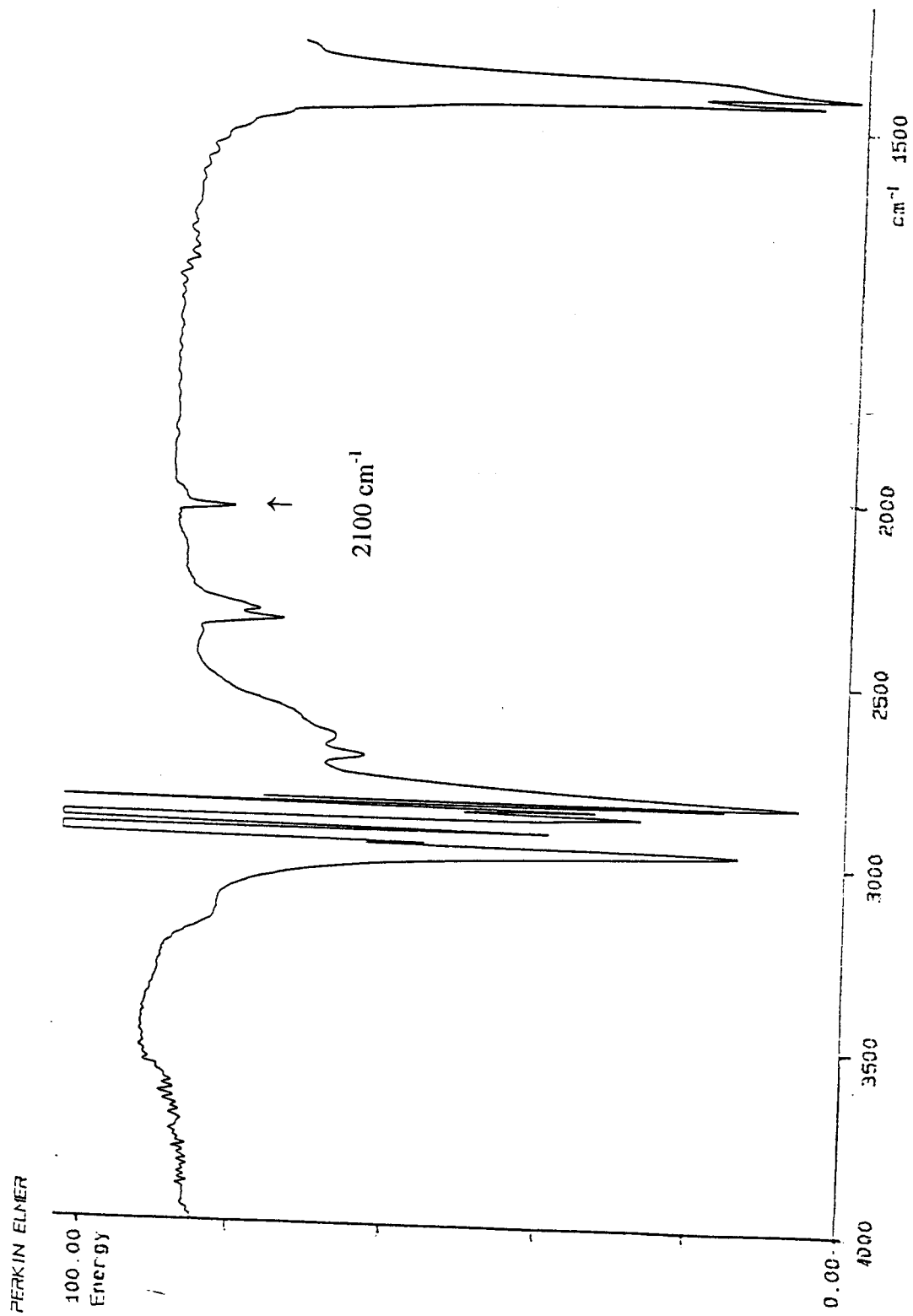


Figure 22. IR of ADAM using mercuric oxide

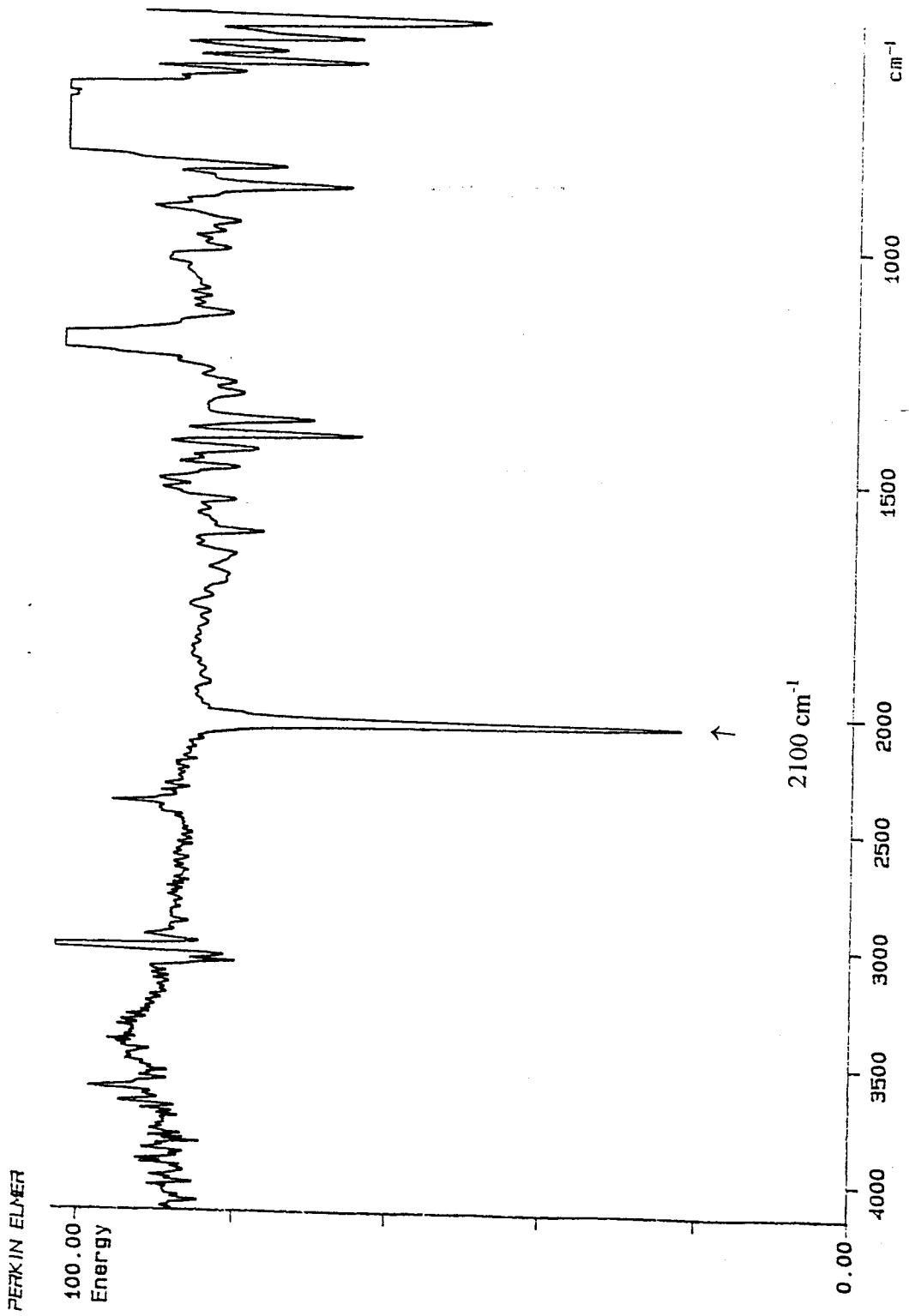
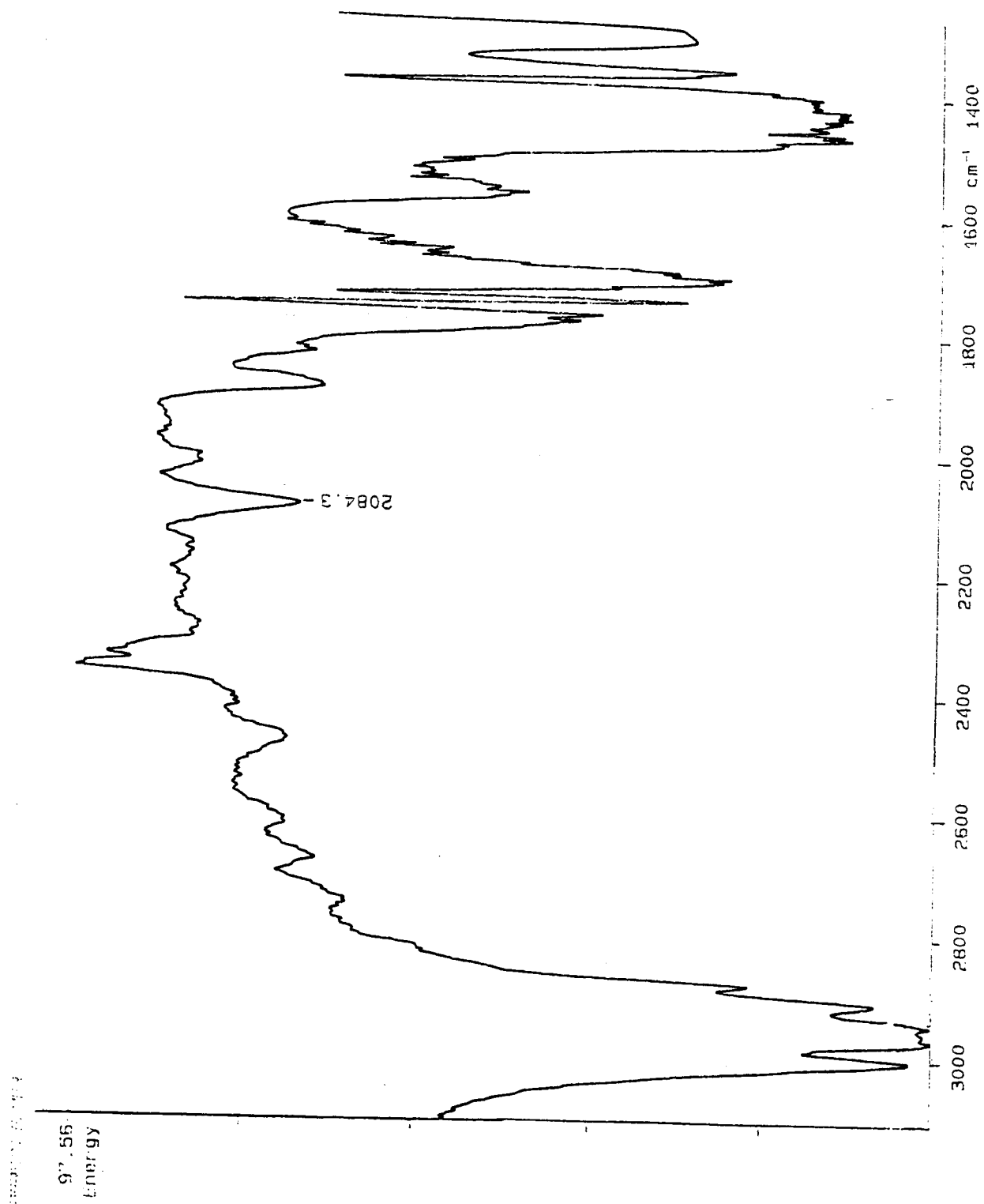


Figure 23. IR of ADAM using NCS



(11). Barker and colleagues added a drop of glacial acetic acid to the reaction mixture at the end of the reaction to decompose excess ADAM. Therefore, pure ADAM must be the spot at the origin of the TLC plates.

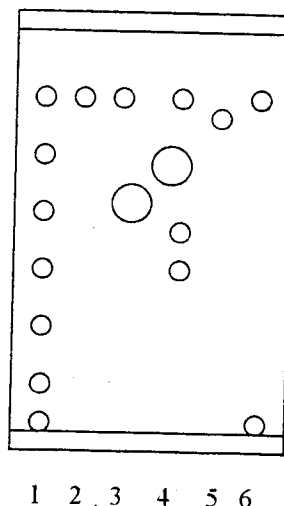


Figure 24. TLC of ADAM and anthracene compounds: ADAM by the mercuric oxide method (1), 9-anthraldehyde (2), 9-anthraldehyde hydrazone (3), 9-anthracene methanol (4), 9-methylanthracene (5), and ADAM by the NCS method (6)

### Part C: Purification of Crude ADAM

Since the ADAM synthesized by the mercuric oxide method still contained several impurities, column chromatography, sublimation, and HPLC were used in an attempt to purify the crude ADAM.

Gravity and flash column chromatography were used based on methods given in the literature dealing with purification of diazo compounds. House *et al.* (27) used a florisil column. Weingarten *et al.* (28), Popic *et al.* (29), and Sekiguchi *et al.* (30) used flash silica gel chromatography. Woolsey *et al.* (31) and Dion *et al.* (32) used a basic or neutral alumina column. The florisil and silica columns separated the impurities but some

yellow color stayed at the top of the column. When the sample was added to the top of the column and it reached the florasil and the silica, bubbles were given off. This is thought to be nitrogen gas evolving indicating that ADAM may have reacted with the stationary phase. This yellow product could not be eluted out with the variety of solvents tried. No bubbles were seen with calcium carbonate and neutral alumina, however, separation was not complete. The IR spectra showed a small diazo peak in many of the fractions which also contained several impurities based on TLC.

Yates *et al.* (33) used sublimation to purify diazo compounds. This technique was used, however, the sublimed material did not give a diazo band on the IR and many impurities still remained in the original sample.

Figure 25 shows an HPLC chromatogram of ADAM from mercuric oxide using 100 % acetonitrile at a flow rate of 0.4 mL/min with the UV detector at 256 nm.

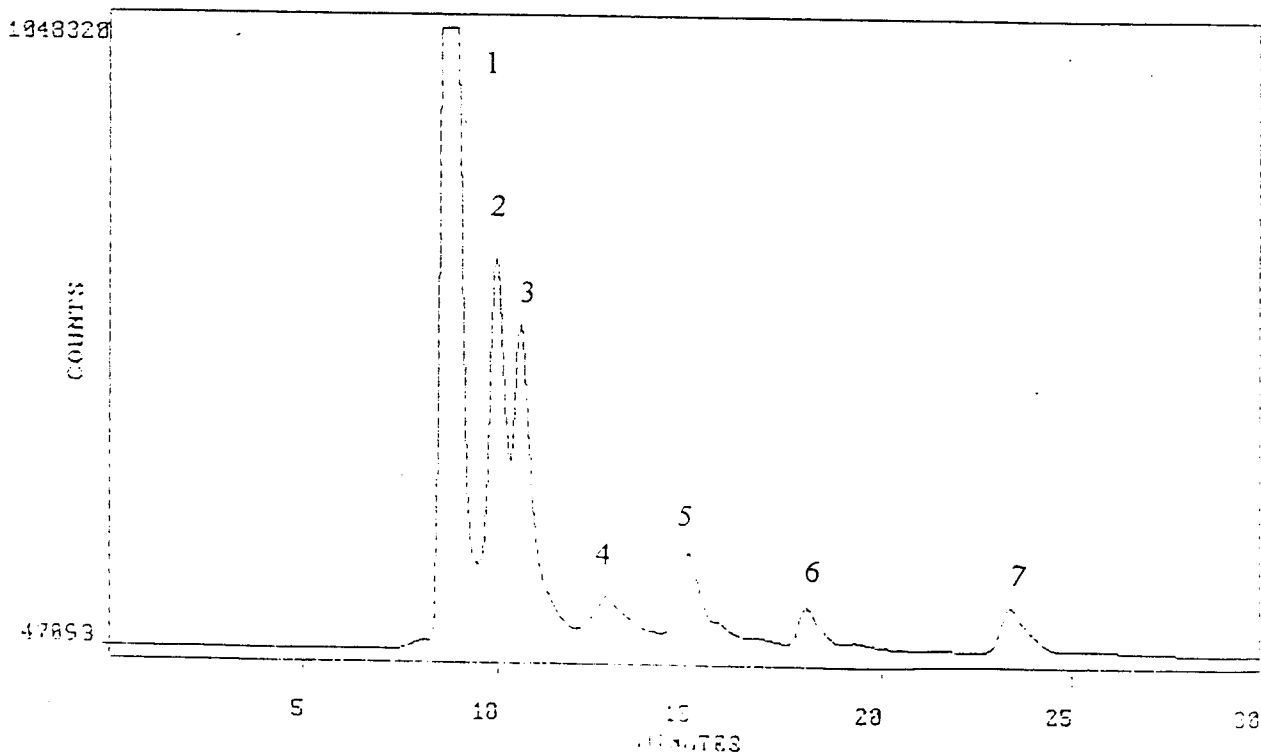


Figure 25. HPLC of ADAM

**Part D: Experiments with Synthesized ADAM**

The ADAM synthesized by the mercuric oxide and NCS methods reacted with stearic acid to give an extra fluorescent spot on the TLC plate. This is evidence that ADAM is present in a high enough concentration for reaction with fatty acids.

Rotovapped HPLC peaks # 1, 2, and 3 did not produce an extra spot on the TLC when reacted with stearic acid which confirms that fractions 1, 2, and 3 are not ADAM. Fractions 4-7 were still impure, showing several spots on the TLC plate.

Silica gel, HCl, and pyridine-HCl were used to protonate the phosphate group on AMP (sodium salt). A crown ether (18-crown-6) was used as a phase transfer catalyst and to surround the sodium ions paired to the negative oxygen on the phosphate group of AMP. Also, various solvents, namely THF, DMPU, methylene chloride, and chloroform, were tried but no identifiable derivative was observed on the TLC.

Acidic AMP was purchased in which the phosphate group was already protonated instead of as a sodium salt. Different pHs, solvents, and concentrations were used, however, no derivative was found.

Also, no derivatives were found when ADAM was reacted with CTP.

## Chapter 5

### Conclusions

A summary of experimental results and conclusions are given in the following four parts.

#### **Part A: Experiments with purchased ADAM**

Reactions with the purchased ADAM failed to produce any concrete evidence for derivatization of AMP or any of the other phosphorylated compounds used. The one case in the reaction between ADAM and AMP at pH 6 in which an extra spot was seen on the TLC plate was not reproducible. Even stearic acid, a fatty acid, did not react with ADAM to form a derivative. Apparently, the purchased ADAM contained a higher concentration of impurities than ADAM itself.

#### **Part B: Synthesis of ADAM**

Among the three methods of synthesis studied, the NCS method resulted in the least number of impurities present on silica TLC plates in 3:2 (v/v) hexane : ethyl acetate. It also showed a strong diazo band at  $2084\text{ cm}^{-1}$  and aromatic bands at  $3000\text{ cm}^{-1}$ . The NCS method was the simplest and the easiest of the three methods. However, it is an *in situ* preparation and once synthesized, it was recommended to use the ADAM immediately in a reaction or store it for up to 24 hours below  $5\text{ }^{\circ}\text{C}$ . On the other hand, the mercuric oxide method provided solid ADAM that can be stored up to several months at  $-76\text{ }^{\circ}\text{C}$ .



The mercuric oxide method proved to give a better yield than the manganese dioxide method but resulted in many more impurities and hydrolyzed products than the NCS method. Although this method was convenient in that solid ADAM could be stored longer than seen with the NCS method, for the TLC plate with the best separation (silica plates in 3:2 (v/v) hexane : ethyl acetate) it was difficult to detect any derivative because of all the impurities present.

#### **Part C: Purification of Crude ADAM**

ADAM synthesized according to the mercuric oxide method, underwent several purification techniques. Purification by column chromatography was extremely difficult and may be impossible. The most promising technique seemed to be HPLC with a reverse phase column and a mobile phase of acetonitrile. Investigating the usefulness of a sample preparation column instead of an analytical column may provide a greater concentration of fractionated material to be further analyzed.

#### **Part D: Experiments with synthesized ADAM**

Several explanations can be given for the unsuccessful derivatizations of phosphorylated molecules using ADAM. ADAM synthesized by the mercuric oxide method was in a very small concentration compared with the other impurities and hydrolyzed products present. This may have caused the detection of any derivatives to be difficult. Another reason for unsuccessful derivatizations was different solubilities. Most of the phosphate compounds studied were soluble in highly polar solvents such as water and methanol, where ADAM was more soluble in less polar solvents such as ether or

ethyl acetate. The immiscibility of the solvents may have kept the reaction from occurring since the two reactants cannot come in contact with each other, even in the presence of a crown ether. The insert from Kamiya Biomedical Company states that ADAM can be used with aqueous solutions; however, Dr. Mark Rose from Merck & Co., West Point, PA. suggested that ADAM may be destroyed by any water present in the reaction mixture.

We believe another reasonable explanation may involve the resonance stability of the monophosphate. We began this study assuming the monophosphates would behave in an identical fashion to phosphonates. This may not be the case. Macomber (14) proved that a phosphonic acid can be esterified by diazomethane. Phosphonates are less resonance stabilized than monophosphates (Figure 26) and therefore react readily with diazomethane. The phosphate group may have a high degree of resonance stability and may not act as a good nucleophile.

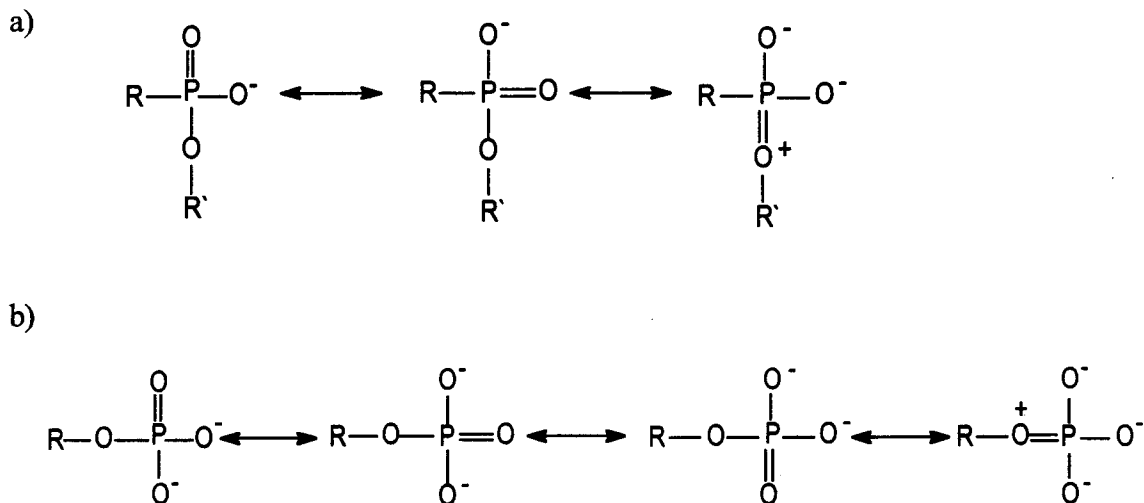


Figure 26. The resonance structures of a) phosphonates and b) monophosphates

Even though our results were inconclusive and sometimes confusing, we are still hopeful that future experiments with ADAM prepared by the NCS method will lead to success. The NCS method was the easiest and the purest way to obtain ADAM; however, we became aware of it late in our research and only spent a short period of time examining it. Future investigations should include more studies on ADAM prepared by the NCS method and triphosphate nucleotides since they are less resonance stabilized than the monophosphates which were primarily used in this research. Also more phosphorus NMR should be performed to monitor the reaction in order to detect small amounts of a derivative that are not seen on the TLC. Finally, nitrogen NMR could be used to detect how much of the diazo compound (ADAM) is actually present among all the impurities.

## References

1. Kessler, C., ed. Nonradioactive Labeling and Detection of Biomolecules. Springer-Verlag Berlin Heidelberg, 1992. 1-2.
2. Kessler, C., ed. Nonradioactive Labeling and Detection of Biomolecules. Springer-Verlag Berlin Heidelberg, 1992. 12-13.
3. Kessler, C., ed. Nonradioactive Labeling and Detection of Biomolecules. Springer-Verlag Berlin Heidelberg, 1992. 70-73.
4. Langer, P., Waldrop, A., and Ward, D. "Enzymatic Synthesis of Biotin-Labeled Polynucleotides: Novel Nucleic Acid Affinity Probes." Proc. Natl. Acad. Sci. USA **78** (1981): 6633-6637.
5. Howard, G., ed. Methods in Nonradioactive Detection. Connecticut: Appleton and Lange, 1993. 138-139.
6. Nakaya, T., Tomomoto, T., and Imoto, M. "The Syntheses and the Reactions of Anthryldiazomethane and  $\alpha$ -naphthyldiazomethane." Bulletin of Chemical Society Japan **40** (3) (1967): 691-692.
7. Regitz, M. and Maas, G. Diazo Compounds: Properties and Synthesis. Orlando: Academic Press, Inc, 1986. 233-236.
8. "Diazo Compounds," Microsoft (R) Encarta. Copyright © 1994 Microsoft Corporation. Copyright © 1994 Funk and Wagnalls Corporation.
9. Black, T. H. "The Preparation and reactions of Diazomethane." Aldrichimica Acta **16** (1) (1983): 3-10.
10. Carey, F. and Sundberg, R. Advanced Organic Chemistry. Part B: Reactions and Synthesis. 3<sup>rd</sup> ed. New York: Plenum Press, 1990. 133-137.
11. Barker, S., Monti, J., Christian, S., Benington, F., and Morin, R. "9-Diazomethylanthracene as a New Fluorescence and Ultraviolet Label for the Spectroscopic Detection of Picomole Quantities of Fatty Acids by High Pressure Liquid Chromatography." Analytical Biochemistry **107** (1980): 116-123.
12. Yoshida, T., Uetake, A., Murayama, H., Nimura, N., and Kinoshita, T. "Fluorescent Labeling of Amino Acids with 9-Antryldiazomethane and its Application to High Performance Liquid Chromatography." Journal of Chromatography **348** (1985): 425-429.

13. Kawakami, Y., Ohga, T., Shimamoto, C., Satoh, N., and Ohmori, S. "Determination of Free N-acetylamino Acids in Biological Samples and N-terminal Acetylamino Acids of Proteins." Journal of Chromatography **576** (1992): 63-70.
14. Macomber, R. "Esterification of Phosphonic Acids with Diazomethane." Synthetic Communications **7** (6) (1977): 405-407.
15. Levine, I. Physical Chemistry. 4<sup>th</sup> edition. New York: McGraw-Hill Inc., 1995. 716-720, 737-738.
16. Willard, H., Merritt, L., Dean, J., and Settle, F. Instrumental Methods of Analysis. California: Wadsworth Publishing Company, 1988. 102-106, 197-217.
17. Guilbault, G. Fluorescence: Theory and Instrumentation, Practice. New York: Marcel Decker Inc., 1967. 37-125.
18. Becker, R. Theory and Interpretation of Fluorescence and Phosphorescence. Wiley Interscience, 1969. 117-127.
19. Huheey, J., Keiter, E., and Keiter, R. Inorganic Chemistry. Principles of Structure and Reactivity. 4<sup>th</sup> edition. HarperCollins College Publishers, 1993. 26.
20. Hirschlaff, E. Fluorescence and Phosphorescence. New York: Chemical Publishing Co. Inc. 1939. 10-17.
21. Birks, J. Organic Molecular Photophysics. John Wiley and Sons, 1973. 1-3.
22. Davis. Advanced Physical Chemistry. New York: Ronald Pres, 1965. 610-611.
23. Kawakami, Y. and Ohmori, S. "Microidentification of N-Terminal-Blocked Amino Acid Residues of Proteins and Peptides." Analytical Biochemistry **220** (1994): 66-72.
24. Barker, S., Monti, J., Christian, S., Benington, F., and Morin, R. "Preparation of 9-Diazomethylanthracene." Analytical Biochemistry **132** (1983): 456.
25. Carpino, L. "A Simple Preparation of 'Active' Manganese Dioxide from 'Activated' Carbon." Journal of Organic Chemistry **35** (11) (1970): 3971-3972.
26. Yoshida, T., Uetake, A., Yamaguchi, H., Nimura, N., and Kinoshita, T. "New Preparation Method for 9-Anthryldiazomethane (ADAM) as a Fluorescent Labeling Reagent for Fatty Acids and Derivatives." Analytical Biochemistry **173** (1988): 70-74.
27. House, H. and Blankley, C. "Preparation and Decomposition of Unsaturated Esters of Diazoacetic Acid." Journal of Organic Chemistry **33** (1) (1968): 53-60.

28. Weingarten, M. and Padwa, A. "A Practical and Efficient Synthesis of  $\alpha$ -Diazo Alkynyl Substituted Esters." Synlett (1997): 189-190.
29. Popic, V., Korneev, S., Nikolaev, V., and Korobitsyna, I. "An Improved synthesis of 2-Diazo-1,3-diketones." Synthesis **3** (1991): 195-199.
30. Sekiguchi, A. and Ando, W. "Synthesis of Cyclic Silyl Diazo Compounds." Bulletin of Chemical Society Japan **55** (1982): 1675-1676.
31. Woolsey, N. and Khalil, M. "Synthesis and Reactions of 3-Diazo-1,4-diphenyl-4-hydroxy-2-butanone." Journal of Organic Chemistry **37** (15) (1972): 2405-2408.
32. Dion, H., Fusari, S., Jakubowski, Z., Zora, J., and Bartz, Q. "6-Diazo-5-oxo-L-norleucine, A New Tumor-inhibitory Substance. II. Isolation and Characterization." Journal of the American Chemical Society **78** (1956): 3075-3077.
33. Yates, P. and Kronis, D. "Aliphatic diazo compounds. XIV. The synthesis of 7-substituted 3-diazo-2-norbornanones and the infrared and proton and carbon-13 nuclear magnetic resonance spectra of these diazo ketones and their precursors." Canadian Journal of Chemistry **62** (1984): 1751-1766.